Slides for Dose, Dosimetry, and Background Radiation

2024

Units of Radiation Exposure (Dose)

Ionization

Roentgen (R)

A simple measure of ionizations in air, can be equated to soft tissue

$$1\ R = 2.58 \cdot 10^{-4}\ \frac{C}{kg\ \boldsymbol{air}}$$

$$i = \frac{1}{W}\left(-\frac{dT}{dx}\right)$$

Ionization energy

Energy Absorption

$$\mathbf{1}\ \boldsymbol{Gray}\ (\boldsymbol{Gy}) = \mathbf{1}\ \frac{\boldsymbol{J}}{\boldsymbol{kg}}$$

Always start here! Use stopping power, exponential attenuation, neutron reaction rates (scattering, absorption) to calculate energy deposition

SI Units

$$\mathbf{1}\ \boldsymbol{rad} = \mathbf{100}\ \frac{\boldsymbol{erg}}{\boldsymbol{g}}$$

$$\mathbf{1}\ \boldsymbol{Gy} = \mathbf{100}\ \boldsymbol{rad}$$

CGS Units

Increased Risk

$$\mathbf{1}\ \boldsymbol{Sievert}\ (\boldsymbol{Sv}) = \boldsymbol{Q} * \boldsymbol{Gy}$$

Neither types of radiation, nor types of tissue, respond the same

Use *Quality factor (Q)* to convert Gy → Sv

REM (Roentgen equivalent man)

$$\mathbf{1}\ \boldsymbol{Sv} = \mathbf{100}\ \boldsymbol{rem}$$

Dose Quality Factors

Table 12.1 Dependence of Quality Factor Q on LET of Radiation as Formerly Recommended by ICRP, NCRP, and ICRU

LET (keV μm^{-1} in Water)	Q
3.5 or less	1
3.5–7.0	1–2
7.0–23	2–5
23–53	5–10
53–175	10–20
Gamma rays, X rays, electrons, positrons of any LET	1

Table 12.2 Dependence of Quality Factor Q on LET as Currently Recommended by ICRP, NCRP, and ICRU

LET, L (keV μm^{-1} in Water)	Q
<10	1
10–100	$0.32L-2.2$
>100	$300/\sqrt{L}$

Table 12.3 Principal Elements in Soft Tissue of Unit Density

Element	Atoms cm^{-3}
H	5.98×10^{22}
O	2.45×10^{22}
C	9.03×10^{21}
N	1.29×10^{21}

Other Quality Factors

Table 9.1. Values of the quality factor for different radiations. Source: ICRP [1991]; NCRP [1993].

Radiation	QF
X, γ, $\beta^{\pm}$, (all energies)	1
Neutrons < 10 keV	5
10–100 keV	10
0.1–2 MeV	20
2– 20 MeV	10
> 20 MeV	5
Protons (> 2 MeV) [ICRP]	5
Protons (> 2 MeV) [NCRP]	2
Alpha particles	20

Tissue Weighting Factors

- Different tissues respond differently to the same dose and exposure
- Why do you think this is so?

Tissue or Organ	w_T
Gonads	0.20
Bone marrow (red)	0.12
Colon	0.12
Lung	0.12
Stomach	0.12
Bladder	0.05
Breast	0.05
Liver	0.05
Esophagus	0.05
Thyroid	0.05
Skin	0.01
Bone surface	0.01
Remainder*	0.05

Calculating Dose in Sieverts

Effective dose to one organ

Dose in Gray

$$H_T = \sum_R w_R D_{T,R}.$$

Dose to tissue

Radiation weight integral

$$w_R \cong \overline{Q} = \frac{1}{D} \int_0^\infty Q(L) D(L)\, dL,$$

Quality at energy L

Dose at energy L

Effective dose to whole body

$$E = \sum_T w_T H_T = H_T \sum_T w_T = H_T,$$

Tissue weighting factor

Example Calculation

Example

During the year, a worker receives 14 mGy externally from uniform, whole-body gamma radiation. In addition, he receives estimated 50-y "committed" doses of 8.0 mGy from internally deposited alpha particles in the lung and 180 mGy from beta particles in the thyroid. (a) What is the effective dose for this worker? (b) How much additional external, uniform, whole-body gamma dose could he receive during the year without technically exceeding the NCRP/ICRP annual limit? (c) Instead of the gamma dose in (b), what additional committed alpha-particle dose to the red bone marrow would exceed the annual effective-dose limit?

Example Calculation

(a) Using the radiation weighting factors from Table 14.1, we obtain the following equivalent doses for the individual tissues, with the tissue weighting factors from Table 14.2 shown on the right:

$$H_{\text{Lung}} = 8.0 \times 20 = 160 \text{ mSv} \quad (w_{\text{T}} = 0.12) \tag{14.10}$$

$$H_{\text{Thyroid}} = 180 \times 1 = 180 \text{ mSv} \quad (w_{\text{T}} = 0.05) \tag{14.11}$$

(b) In order not to exceed the annual limit, any additional effective dose must be limited to $50 - 42 = 8$ mSv. Therefore, an additional uniform, whole-body gamma dose of 8 mGy would bring the worker's effective dose to the annual limit of 50 mSv.

The effective dose is, by Eq. (14.4),

$$E = 160 \times 0.12 + 180 \times 0.05 + 14 \times 1 = 42 \text{ mSv}. \tag{14.13}$$

Free Air Ioniazation Chamber

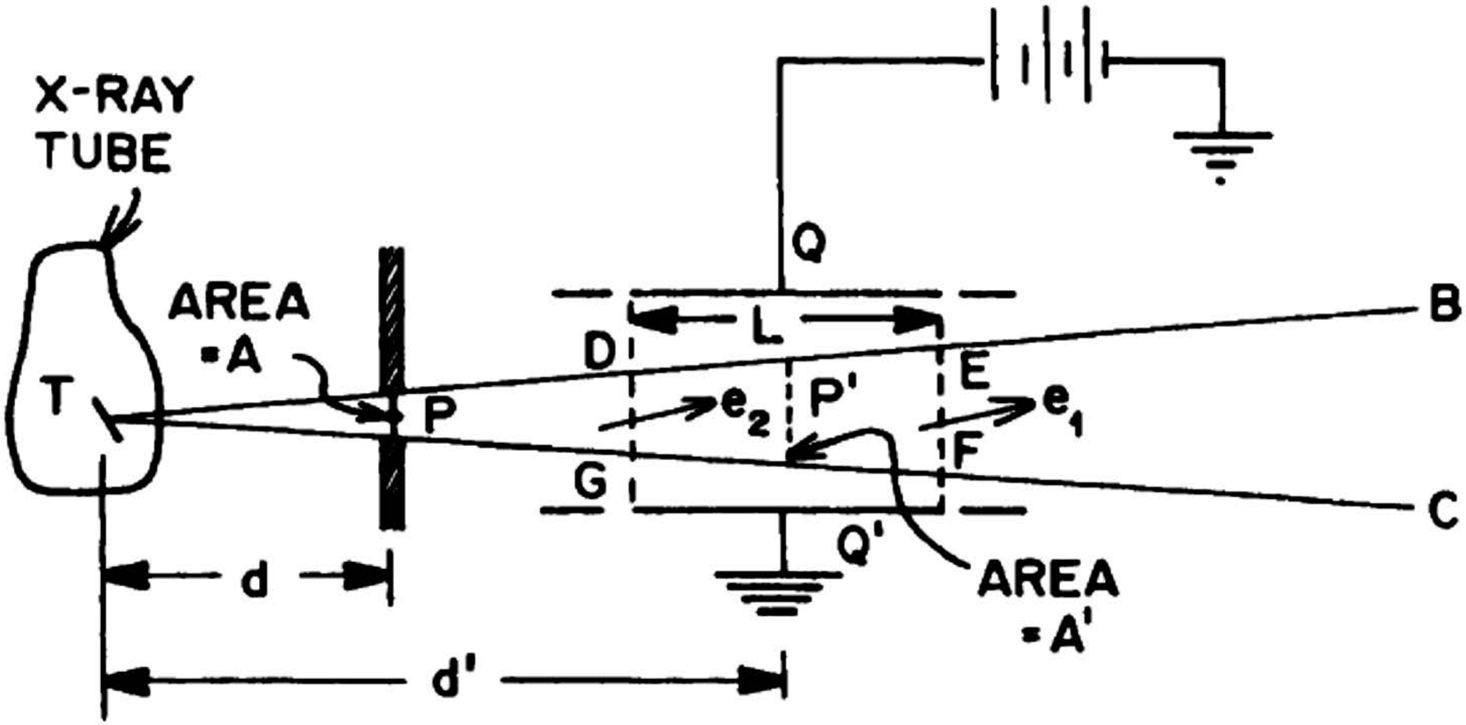

Fig. 12.1 Schematic diagram of the "free-air" or "standard" ionization chamber.

Air-Wall Chambers

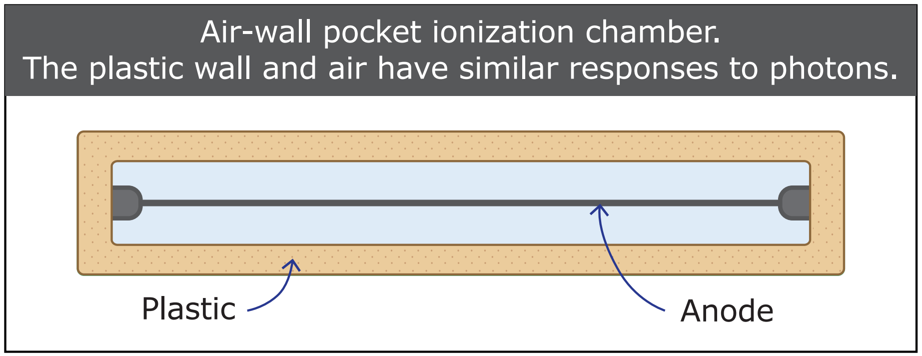

Image by MIT OpenCourseWare.

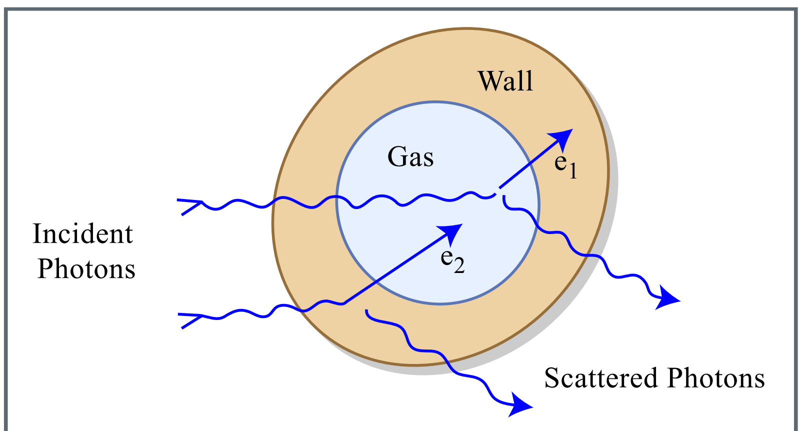

Gas in Cavity Enclosed by Wall to Illustrate Bragg-Gray Principle

Figure by MIT OCW.

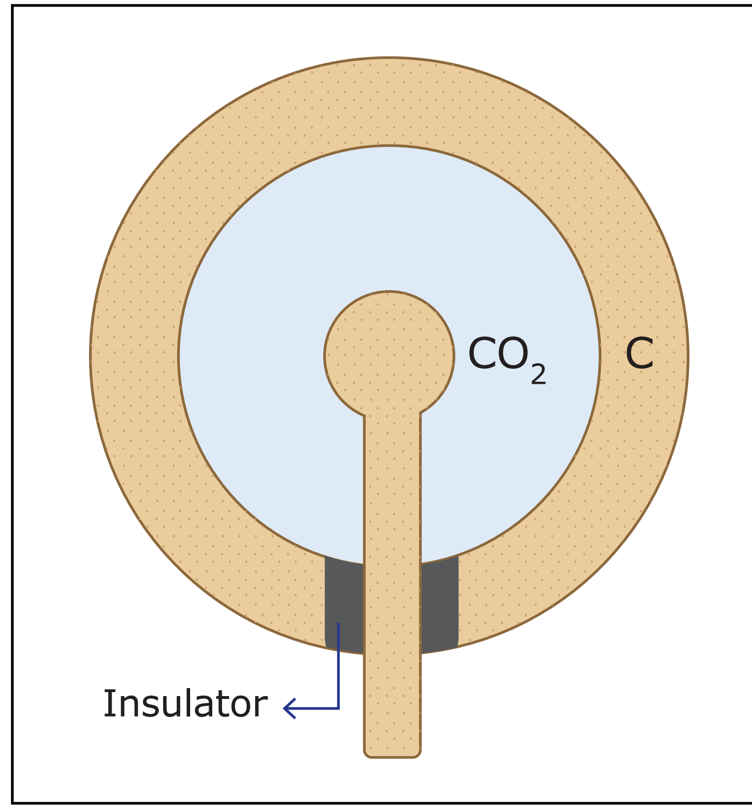

Image by MIT OpenCourseWare.

Air Wall Chambers – Civil Defense

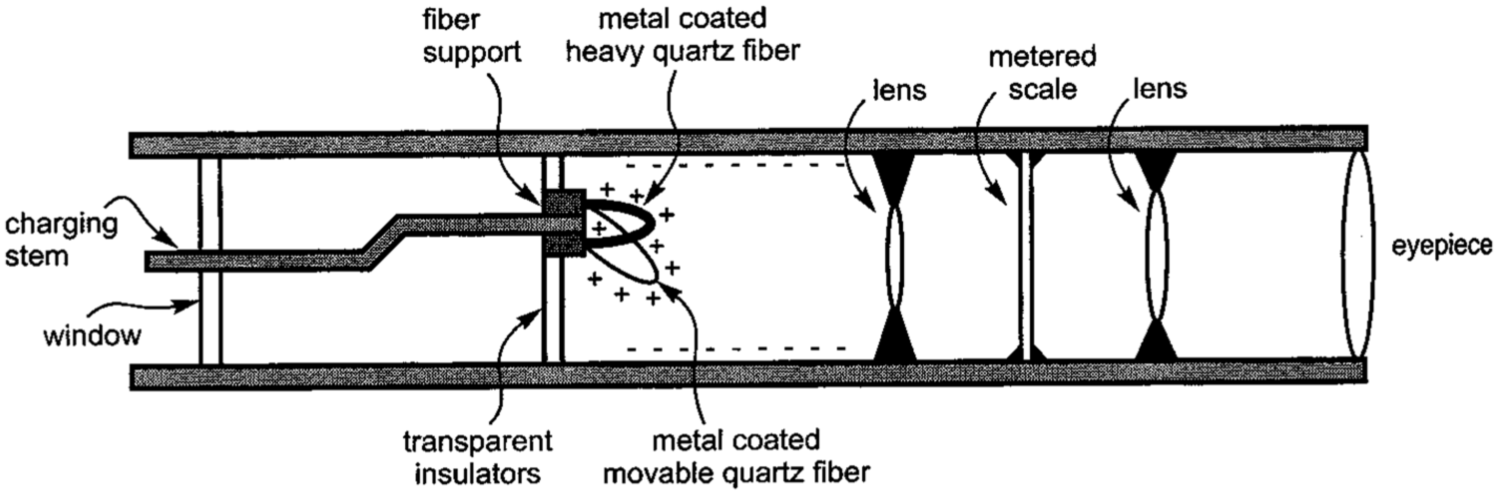

Figure 8.23. The basic components of a pocket ion dosimeter. The quartz fibers are both positively charged and become separated from the Coulombic force. Electrons excited by radiation interactions in the chamber are attracted to the quartz fibers and reduce their charge. As a result, the mobile fiber moves and its position is visually seen on the metered scale.

Air Wall Chambers – Civil Defense

https://www.orau.org/ptp/collection/civildefense/cdv742.htm

http://forums.ubi.com/showthread.php/474129-Creepy-cold-war-souvenir-Forums

Fast Neutron Detector (Tissue Equiv.)

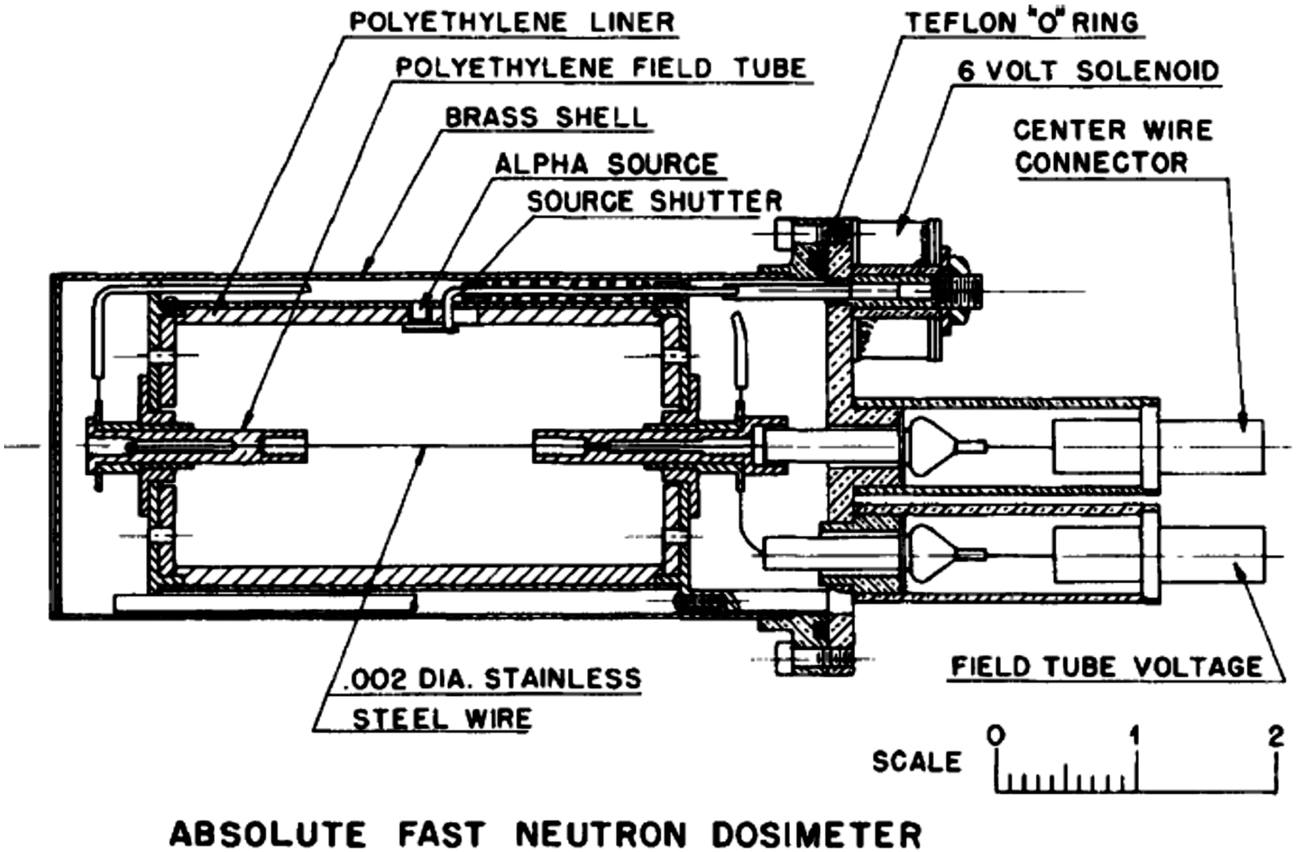

Public domain image, from US DOE.

Ionization (Geiger) Chamber

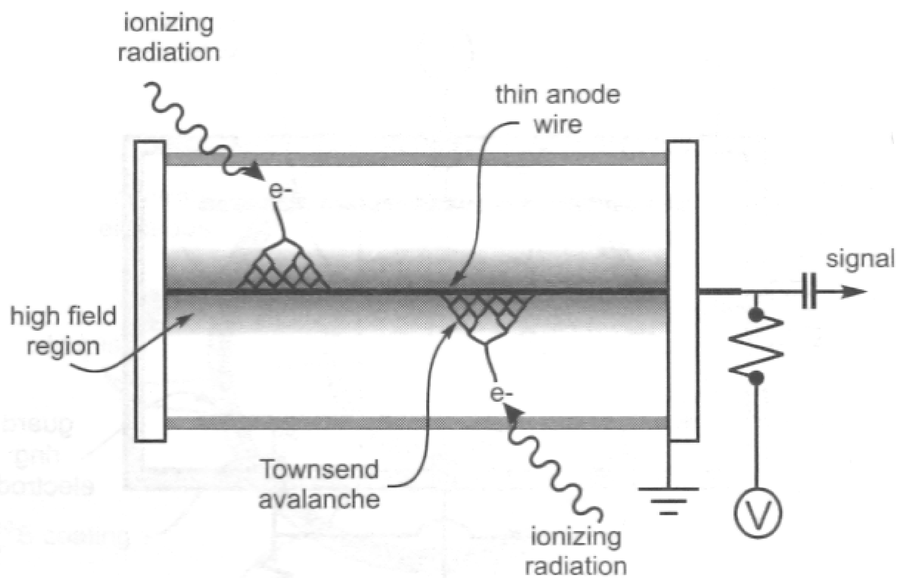

Figure 8.5. With a high electric field near the anode of a gas-filled detector, signal gain is realized through impact or Townsend avalanching, often referred to as "gas multiplication."

Gas Detector Cutaway

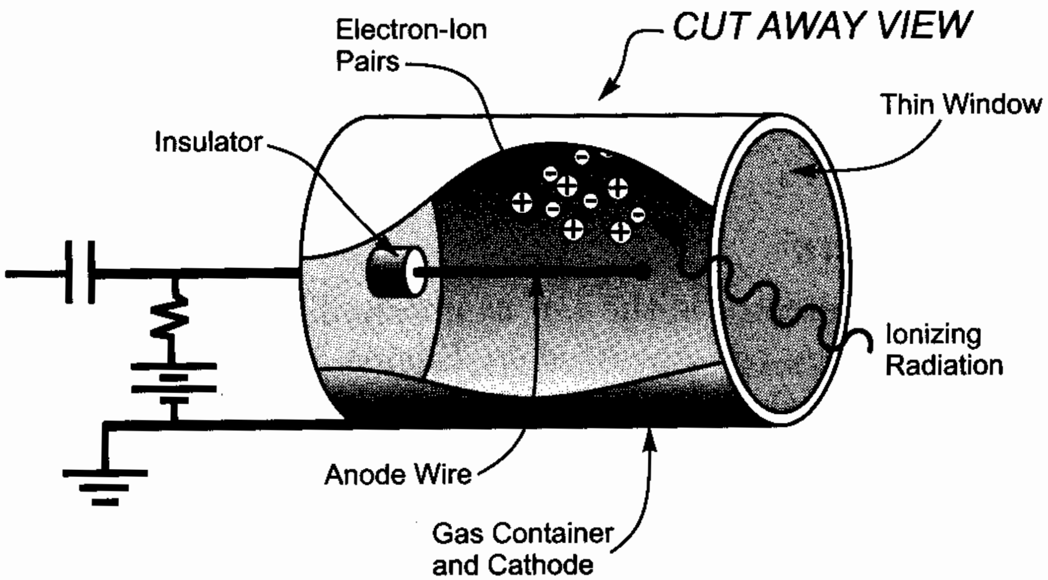

Figure 8.2. Schematic view of a coaxial gas detector, which is commonly used for Geiger-Müller tubes, and sometimes used for proportional counters. High voltage is applied to the central wire anode, while the outer cylinder wall, the cathode, is held at ground.

Gaining/Losing Energy Resolution

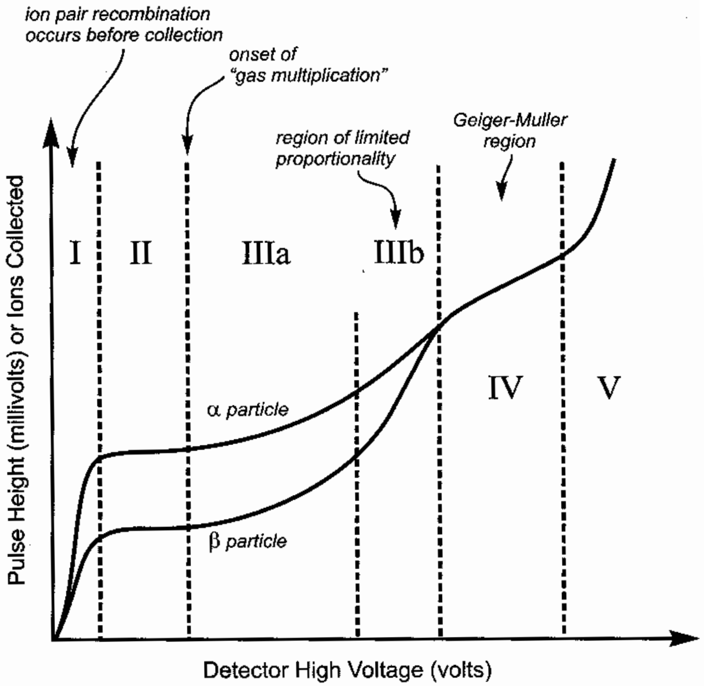

Figure 8.1. The observed output pulse height versus the applied high voltage for a gas-filled detector, showing the main regions: (I) recombination, (II) ion chamber, (III) proportional, (IV) Geiger-Müller, and (V) continuous discharge. This plot is often referred to as the *gas curve*.

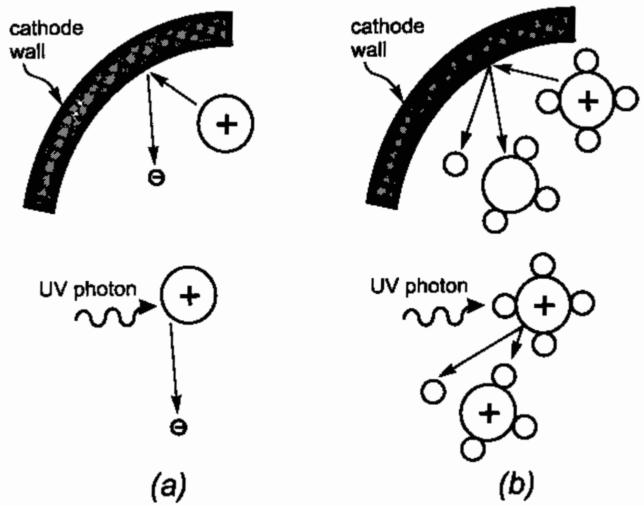

Figure 8.7. A quench gas is used to prevent continuous avalanches in the proportional counter. When an argon ion strikes the cathode wall or absorbs excited UV photons, an electron may be ejected that can start another avalanche, as depicted in *(a)*. The quench gas, usually an organic molecule, breaks apart when it strikes the cathode wall or when it absorbs a UV photon, hence does not release an electron that can start a new avalanche, as depicted in *(b)*.

Combined Gamma/Neutron Detector

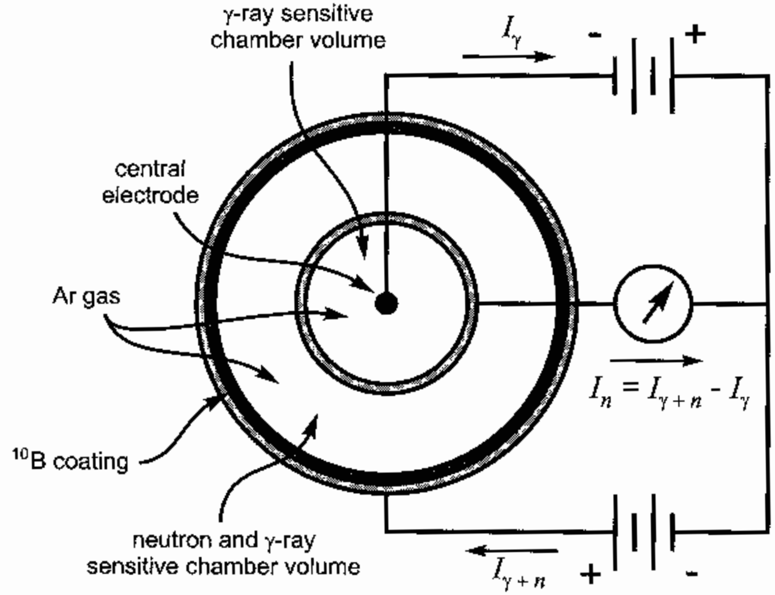

Figure 8.3. Cross section diagram of concentric compensated ion chamber. The configuration allows for both chambers to experience the same radiation field. Differences between the two chambers can be properly calibrated by adjusting the operating voltages.

Occupational Dosimetry – TLDs

https://apps2.campusservices.harvard.edu/ehs/radiation/how_dosimeter.shtml

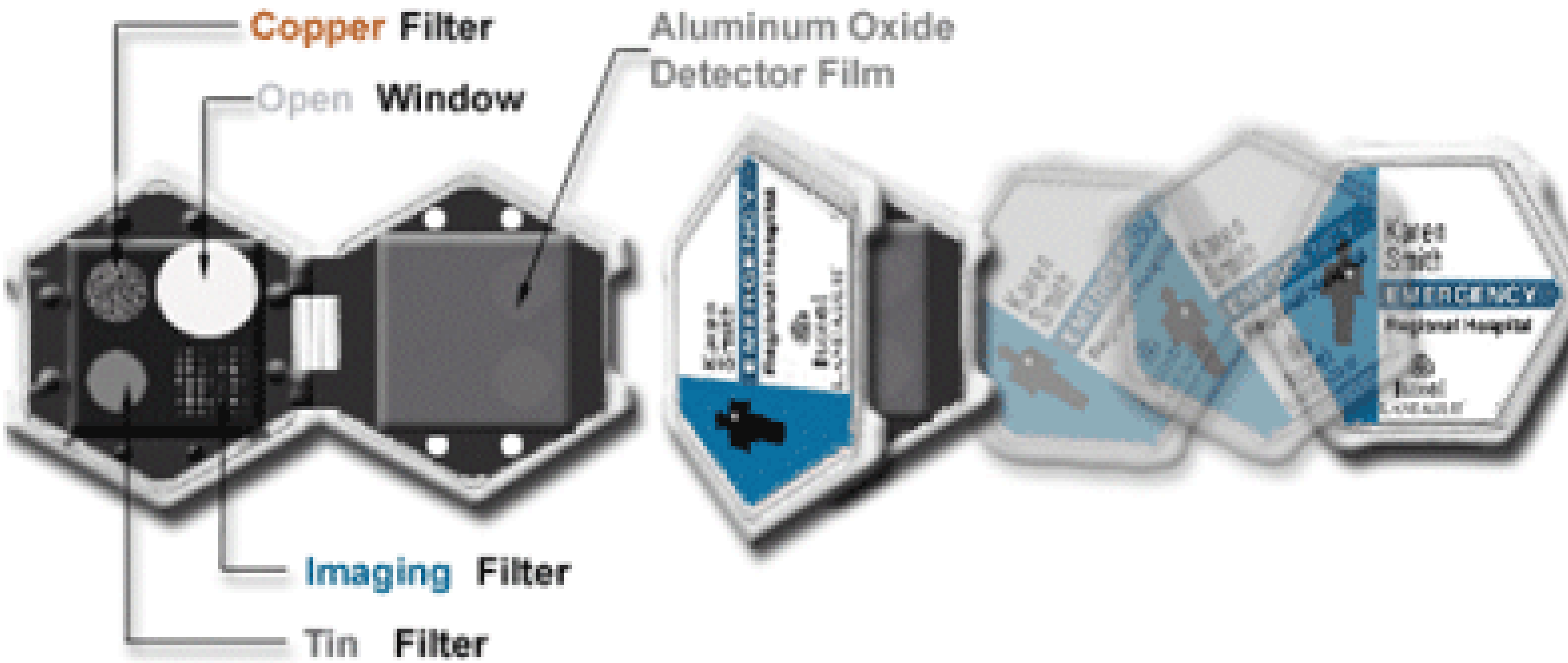

Occupational Dosimetry – TLDs

https://apps2.campusservices.harvard.edu/ehs/radiation/how_dosimeter.shtml

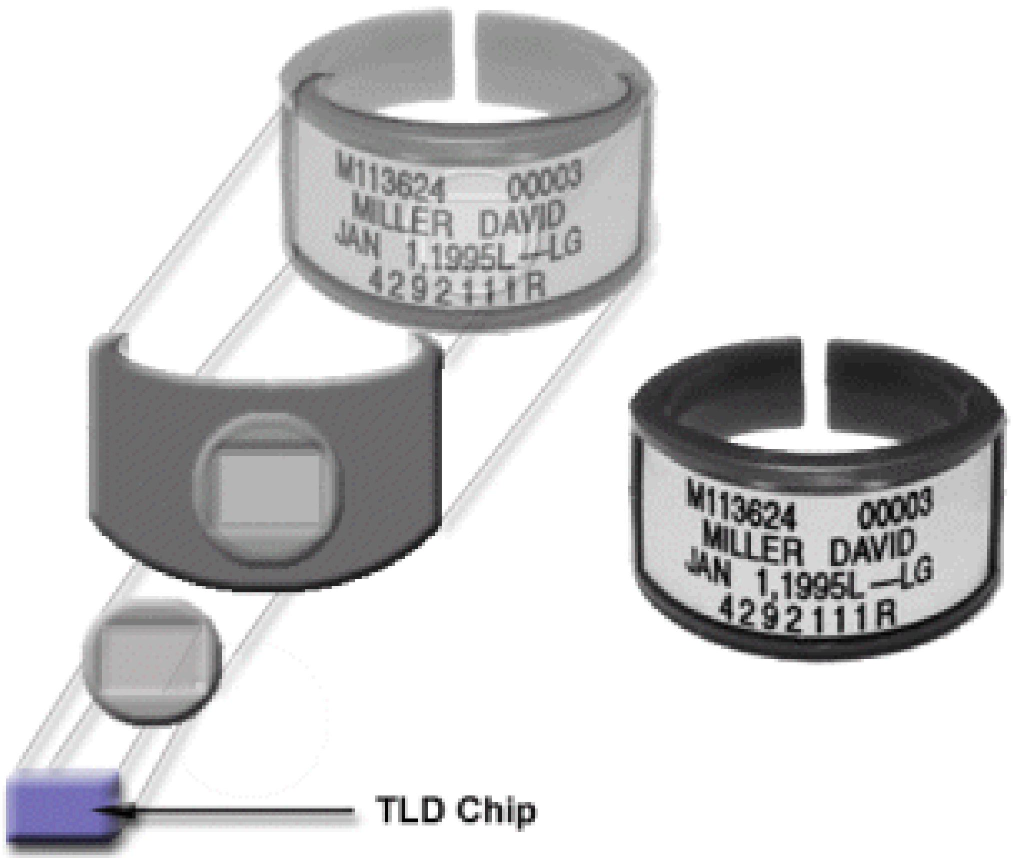

Reading a TLD

L. A. DeWerd, L. Bartol, S. Davis. "Thermoluminescence Dosimetry." *Presentation, AAPM Summer School 2009*, June 24, 2009. Accessed online at www.aapm.org/meetings/09SS/documents/24DeWerd-TLDs.pdf *on 2015-01-16*

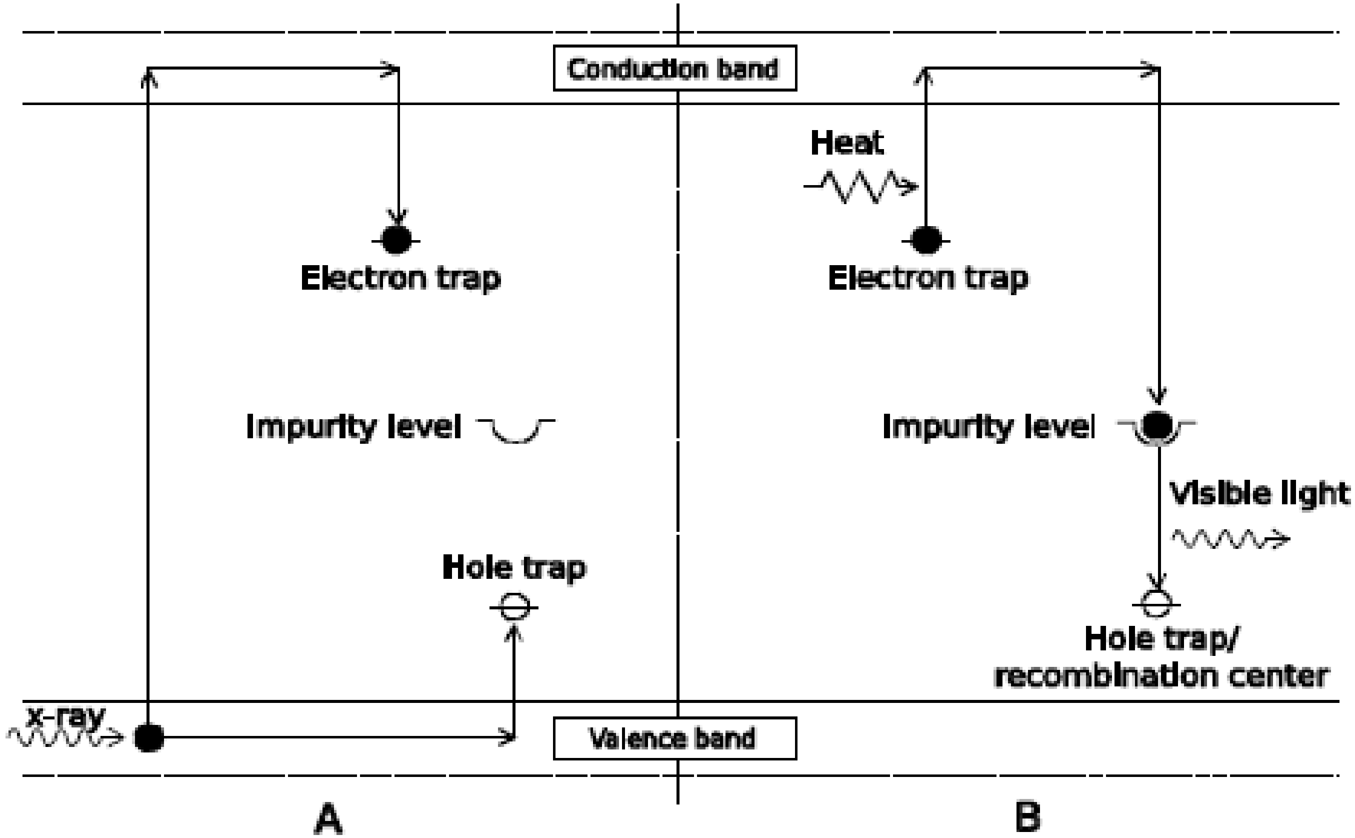

Medical Procedures & Dosimetry

Goal: Destroy tumors, minimize collateral damage to tissue

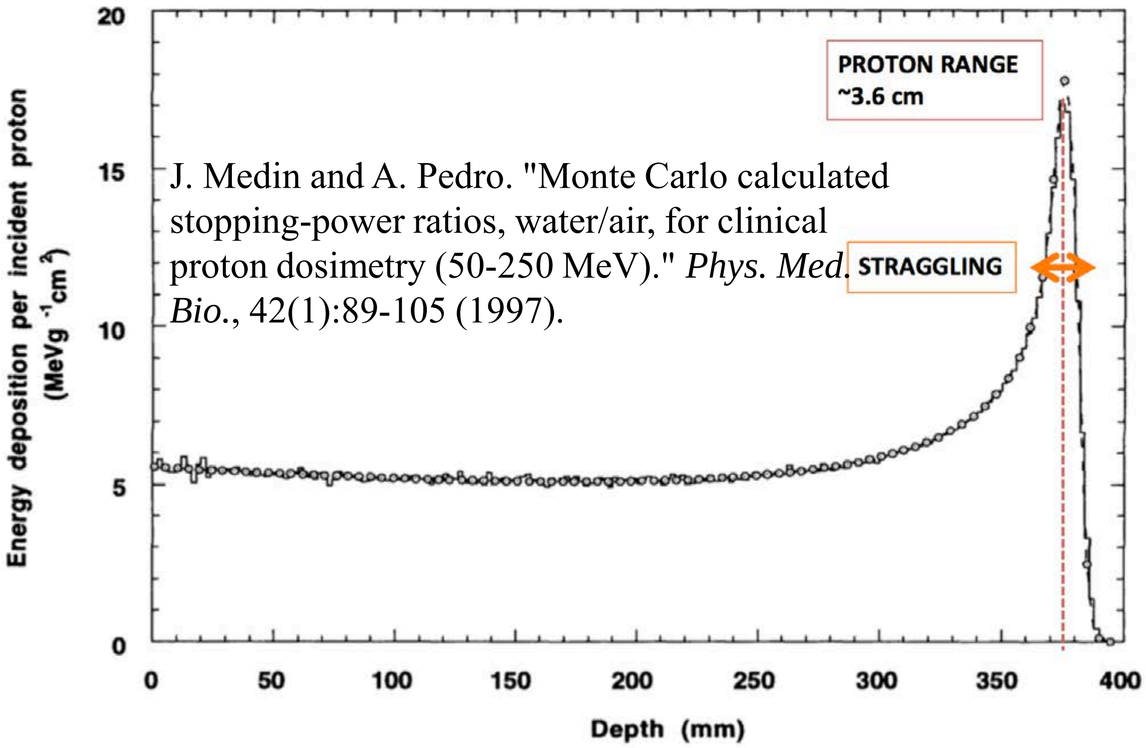

J. Medin and A. Pedro. "Monte Carlo calculated stopping-power ratios, water/air, for clinical proton dosimetry (50-250 MeV)." *Phys. Med. Bio.*, 42(1):89-105 (1997).

Proton Beam Therapy Tricks

W. P. Levin et al. "Proton beam therapy." *British J. Cancer*, 93(8):849-854 (2005).

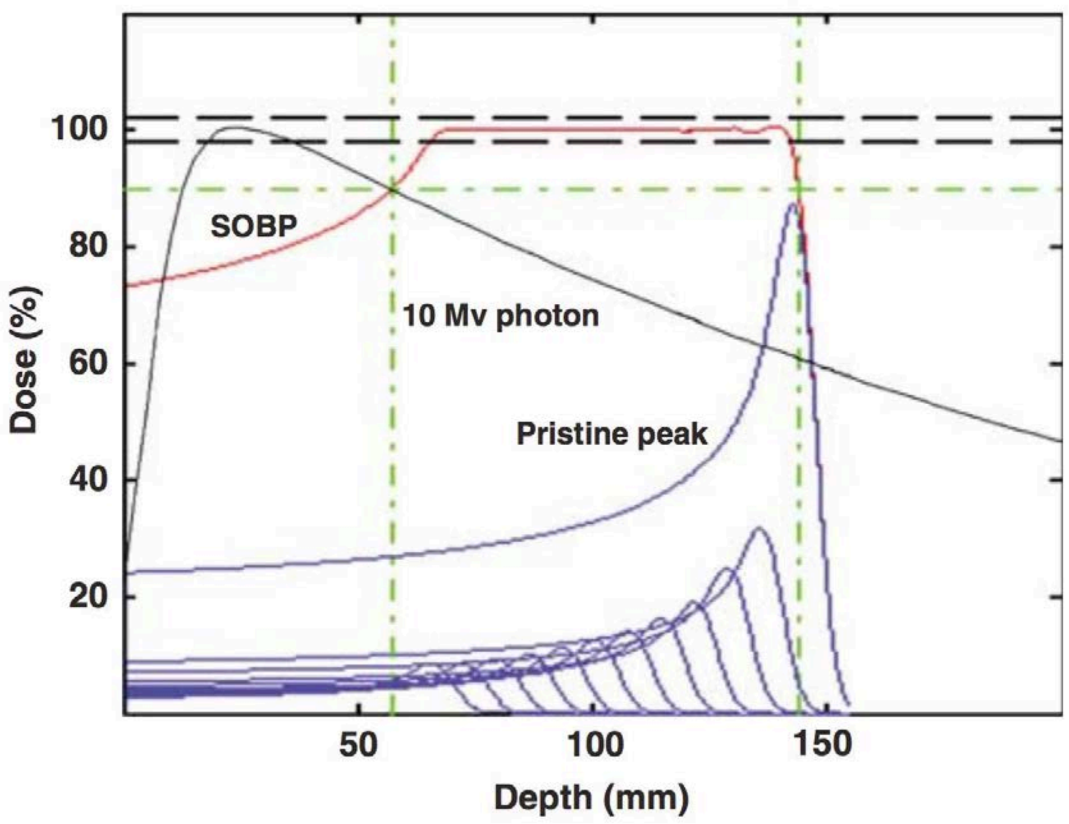

Source: W. P. Levin et al. "Proton beam therapy." *British J. Cancer* 93(8):849-854 (2005).
doi:10.1038/sj.bjc.6602754. License CC BY-NC-SA 3.0.

Problem: Normal Movement

J. M. Balter et al. "Uncertainties in CT-based radiation therapy treatment planning associated with patient breathing." ***Intl. J. Rad. Oncology Bio. Phys.*** **36(1):167 (1996).**

Humans tend to breathe, swallow, digest… moving their organs

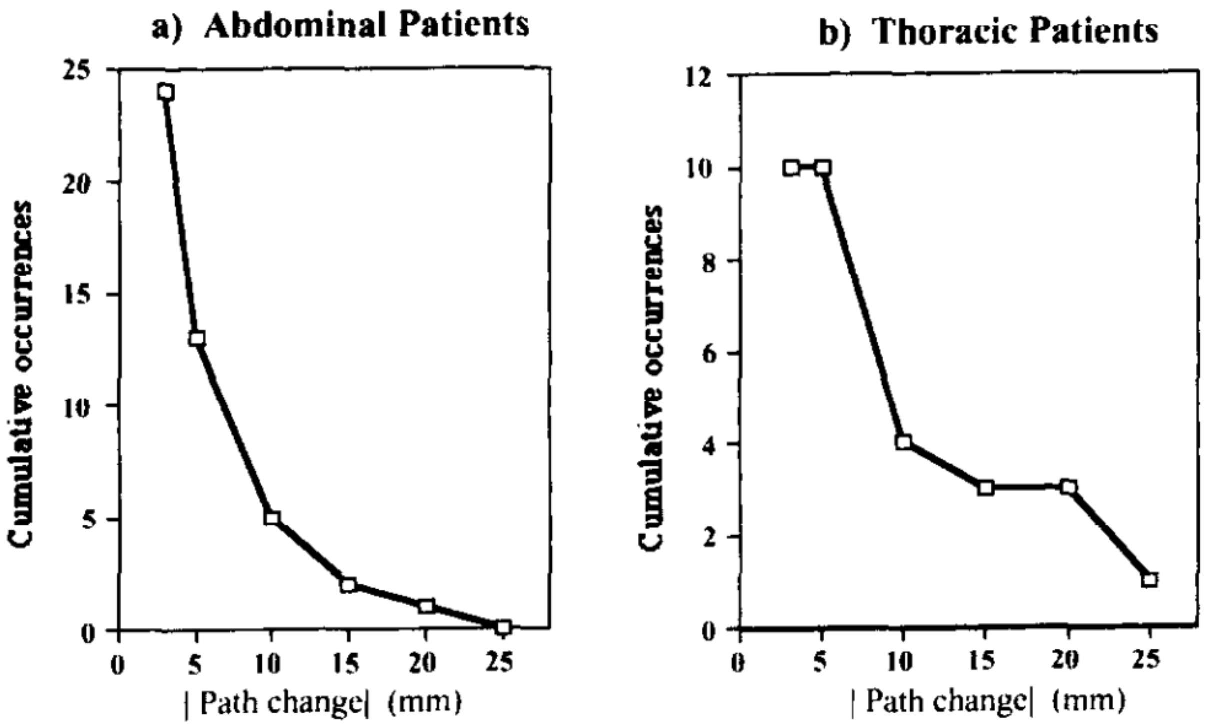

The Ideal IMRT Dosimeter

- The dosimeter can determine absolute dose
- The dosimeter can provide three-dimensional data
- The dosimeter’s response isn’t orientation-dependent
- The dosimeter is well-calibrated, and the interpretation of its readout is rigorously supported by data
- The dosimeter’s ability to measure absolute dose is insensitive to dose rate and energy of the radiation
- The dosimeter is non-toxic
- The dosimeter’s cost to build and maintain is reasonable

Existing Dosimetry Methods

- Monte Carlo calculations
- Conventional port films
- Electronic portal imaging devices (EPID)
- Gel dosimetry
- Electron spin resonance spectroscopy
- Thermoluminescent dosimetry
- Silicon diodes
- Scintillation fibers
- Prompt gamma monitoring
- PET scans
- MOSFET dosimeters

Electronic Portal Imagers (EPID)

http://www.dallasdentalspa.com/digital-radiography.php

Tissue Equivalent Gels

L. J. Schreiner, T. Olding. "Gel Dosimetry." *Presentation, 2009 AAPM Summer School*, Colorado College, CO, USA, June 21-25, 2009.

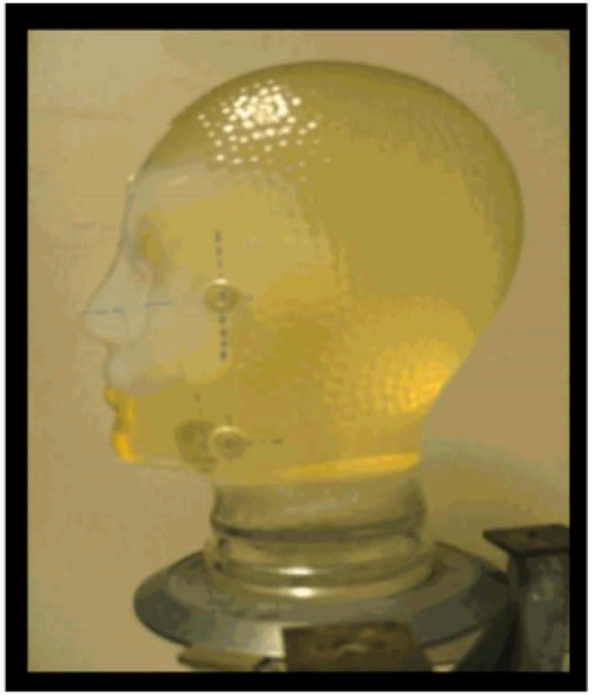

Courtesy of Yves De Deene. Used with permission.

Courtesy of Andrew Jirasek. Used with permission.

Silicon Diodes (Band Gap Change)

TAMU, Nuclear Safeguards Education Portal, "Basic Radiation Detection." Accessible online at http://nsspi.tamu.edu/nsep/courses/basic-radiation-detection/semiconductor-detectors/introduction/introductionwww.aapm.org/meetings/09SS/documents/28Zhu-Diodes.pdf.

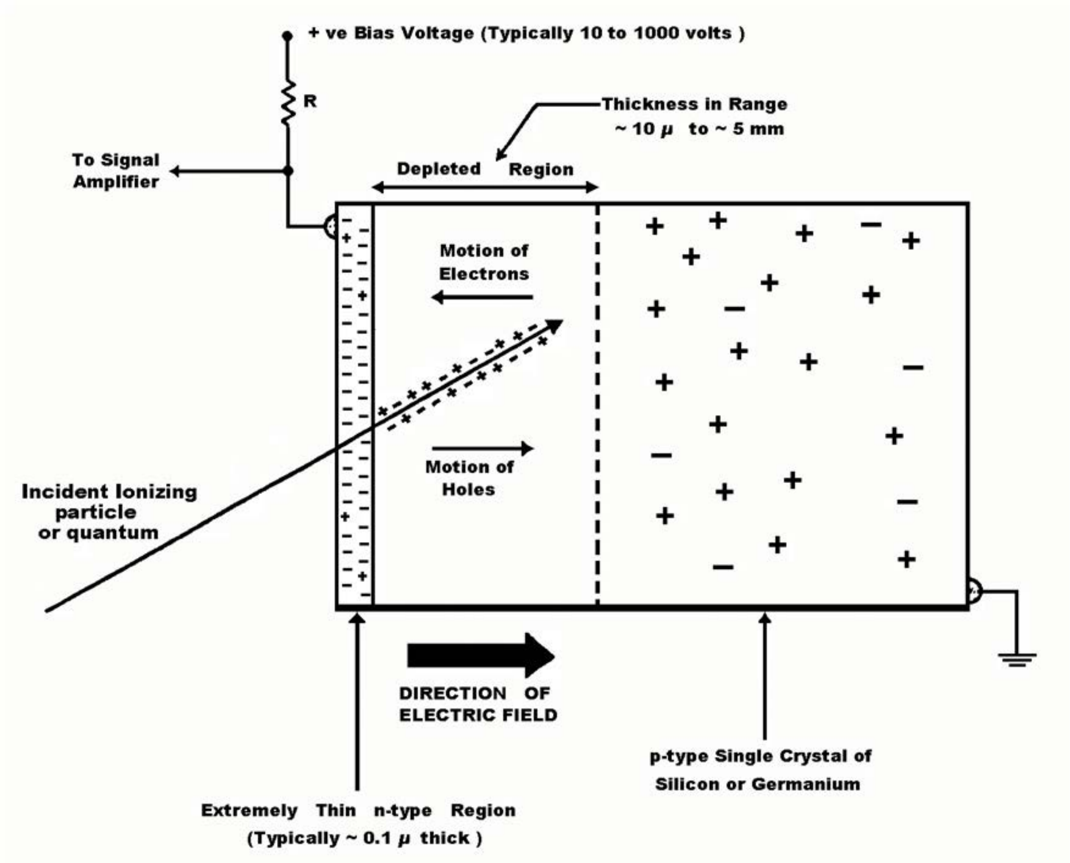

Optically Stimulated Luminescence

M. C. Aznar et al. "Real-time optical-fibre luminescence dosimetry for radiotherapy: physical characteristics and applications in photon beams." *Phys. Med. Bio.*, 49(9):1655 (2004).

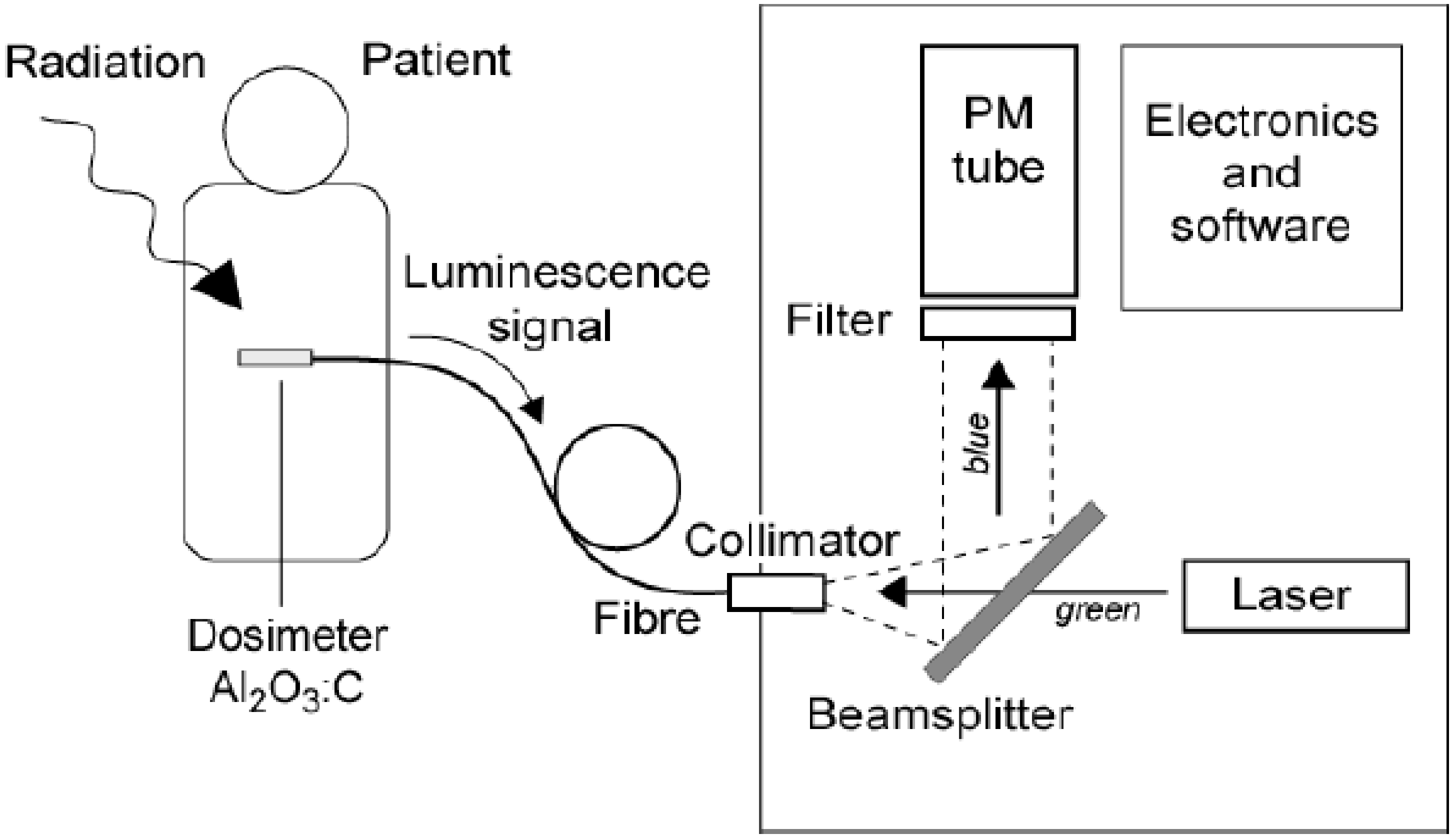

Implanted MOSFETs

G. P. Beyer et al. "Technical evaluation of radiation dose delivered in prostate cancer patients as measured by an implantable MOSFET dosimeter." *Intl. J. Rad. Oncology* Bio.* Phys.*, 69(3):925 (2007).

Significant differences were found to exist between prescribed and delivered cancer therapy treatments!

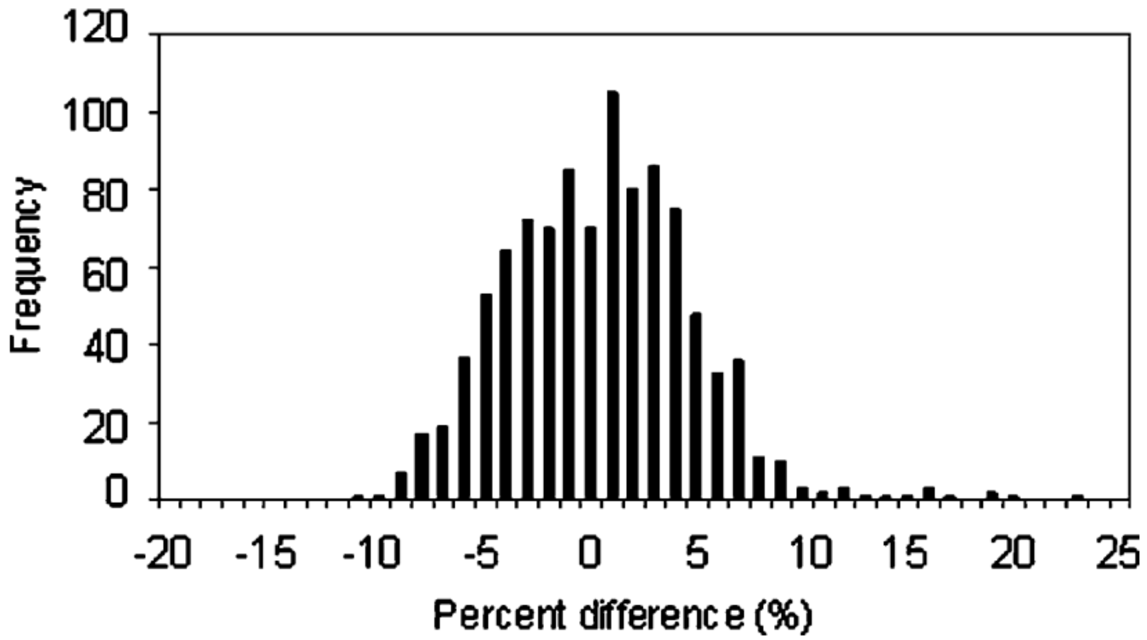

Problems

- Don’t know the real dose to the tumor
- Don’t know the dose to surrounding tissue
- Can’t control the proton accelerator in real time
- Don’t know the dose rate vs. time
- In-situ methods haven’t worked well
- Ex-situ methods don’t tell you real-time information

Our Idea…

The IF^{2}D (Integrating F-Center Feedback Dosimeter)

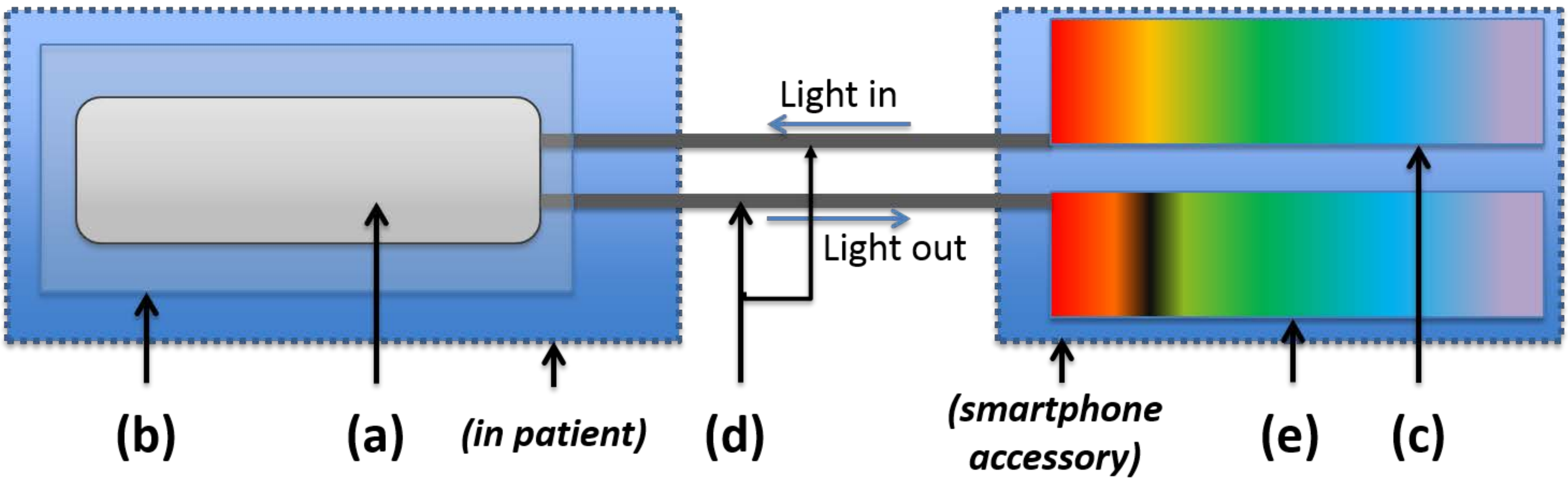

Cody Dennett, Sara Ferry, Dr. Rajiv Gupta (MGH), ***Prof. Michael P. Short***

Presentation ***not given*** to GE Healthcare, MIT International Design Center, Sept. 28, 2016

Methods of Cancer Treatment

Excision

Chemotherapy

X-ray therapy

Brachytherapy

Proton therapy

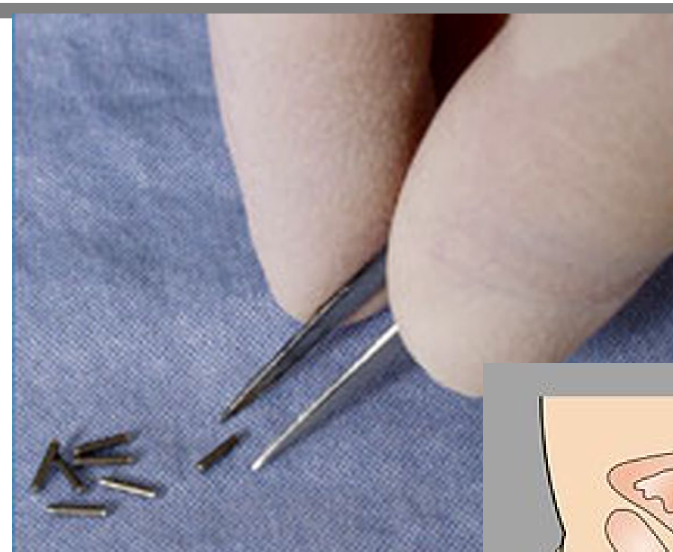

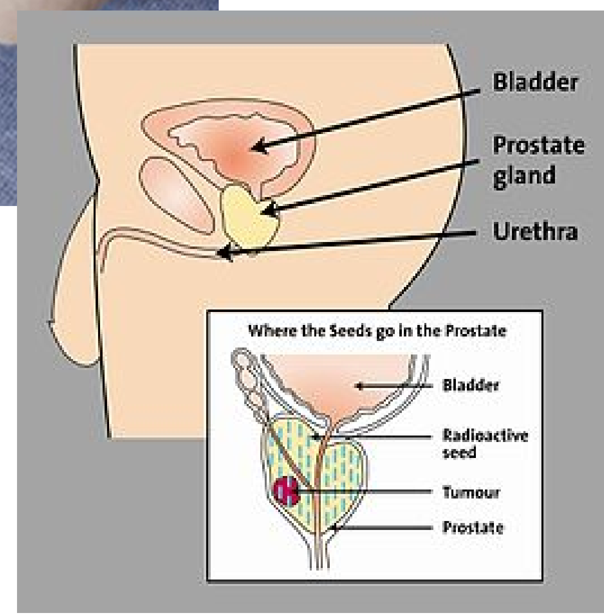

Public domain images

Images: Wikimedia Commons

X-Ray Therapy

http://www.aafp.org/afp/2008/1201/p1254.html

Hinges upon absorption of x-rays by tumors

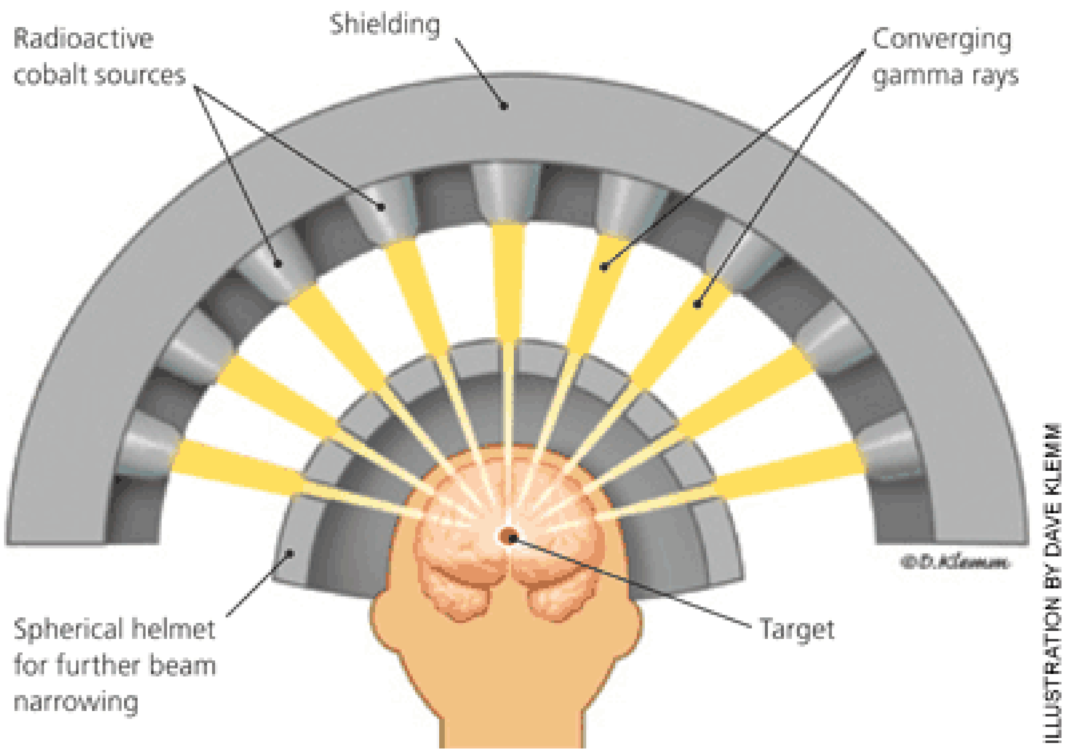

Proton Therapy

http://www.symmetrymagazine.org/article/december-2008/the-power-of-proton-therapy

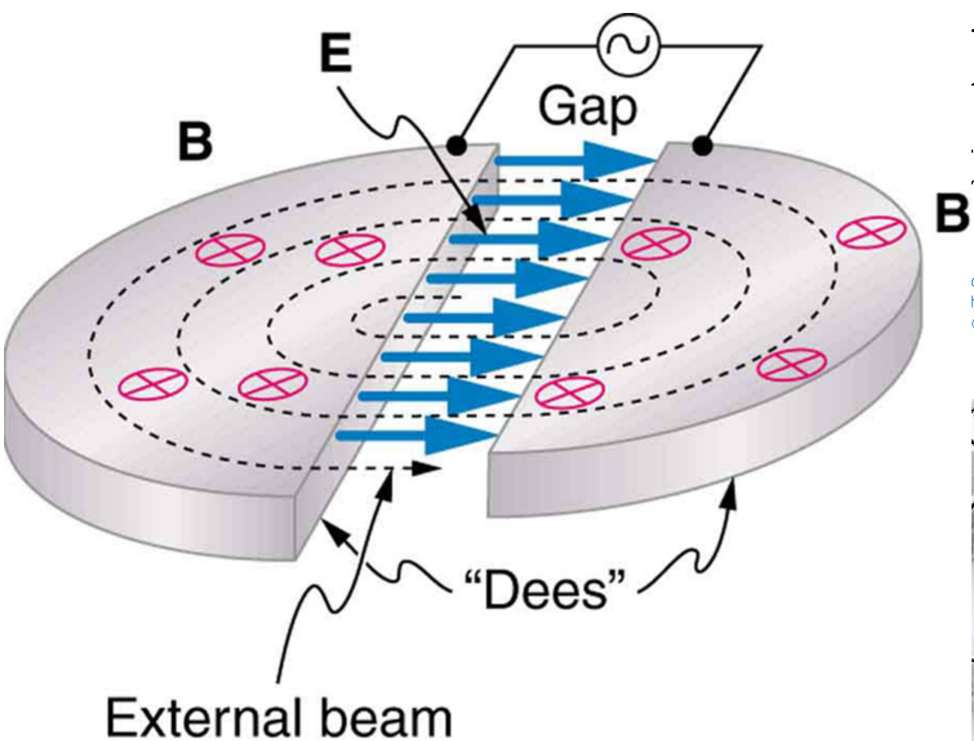

http://voer.edu.vn/m/accelerators-create-matter-from-energy/389d856b

lotron) to accelerate
he tumor!

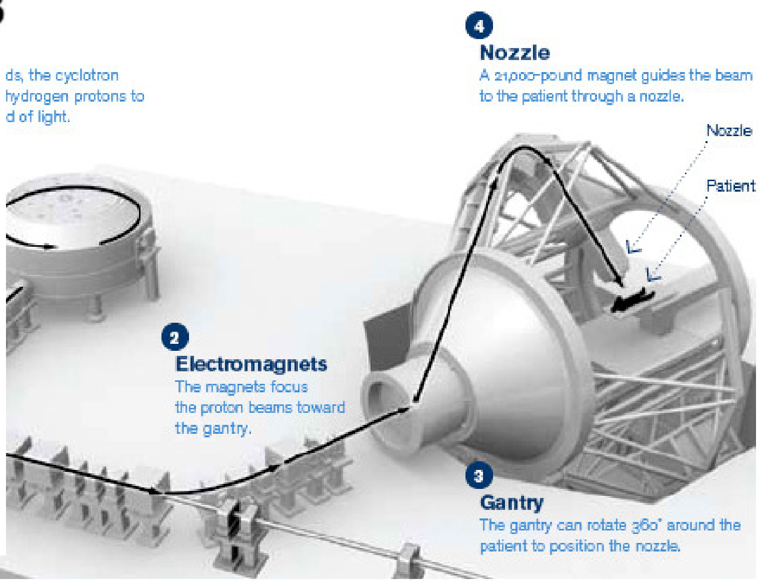

Why Protons vs. X-Rays?

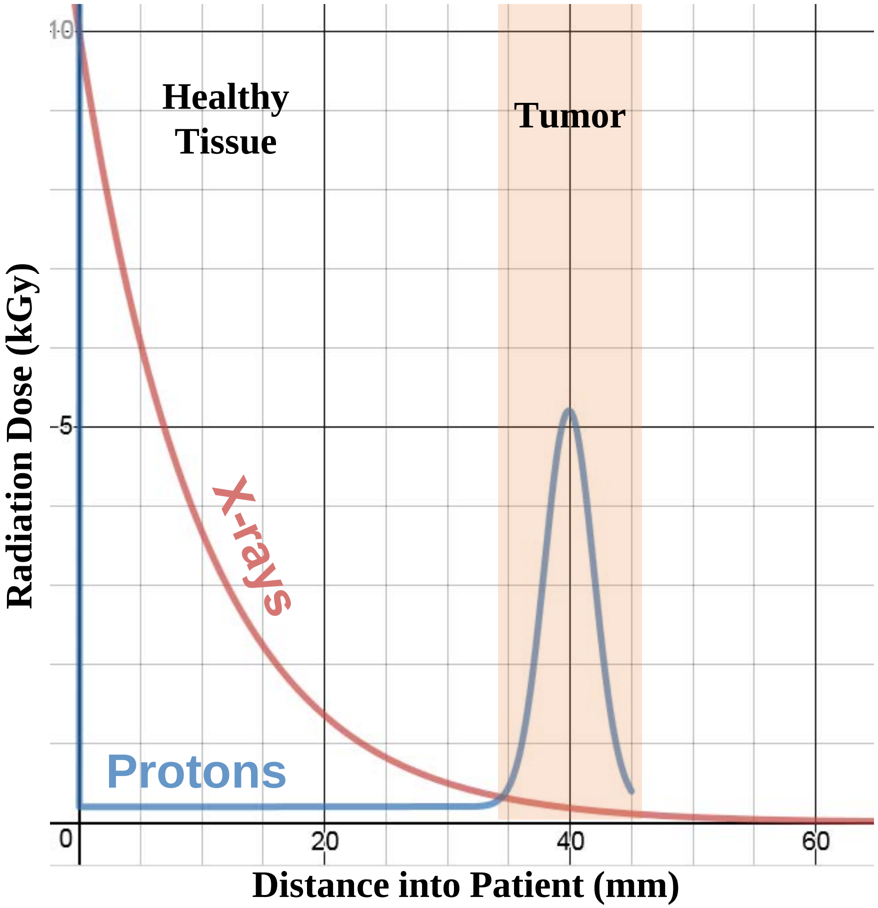

Highly controllable range vs. just attenuation

More dose to tumor, less dose to surrounding tissue

Question: How Can We Sense the Total Dose? The Dose Rate?

The IF^{2}D: The Integrated F-Center Feedback Dosimeter

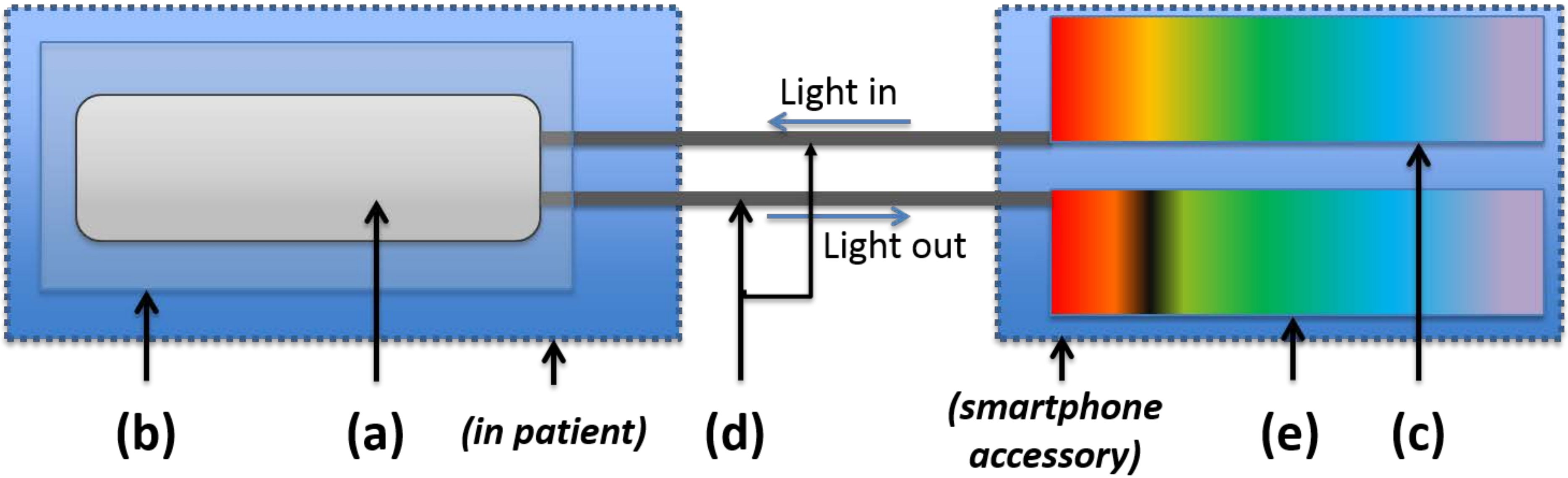

a) F-center active alkali halide salt
b) Biocompatible casing
c) Calibrated white light source
d) Fiber optic connection cables
e) Spectrometer to read absorption

The IF^{2}D Relies on F-Centers

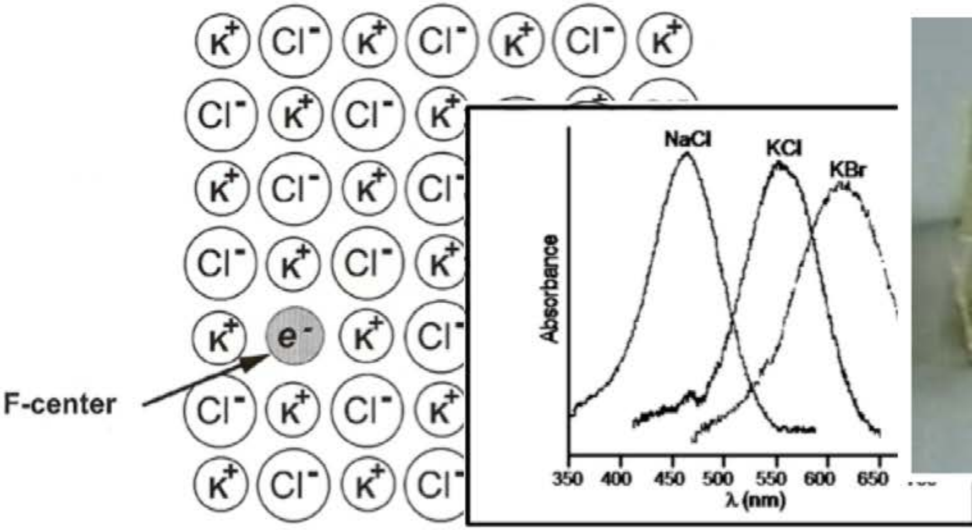

Atomic defects are optically active, absorbing specific wavelengths of light

Crystals of alkali halide salts after exposure to radiation

F-Center Creation vs. Radiation Is Very Well Known

Sodium chloride after irradiation with 30 kV and 50 kV x-rays. The open circles show experimental absorption measurements.

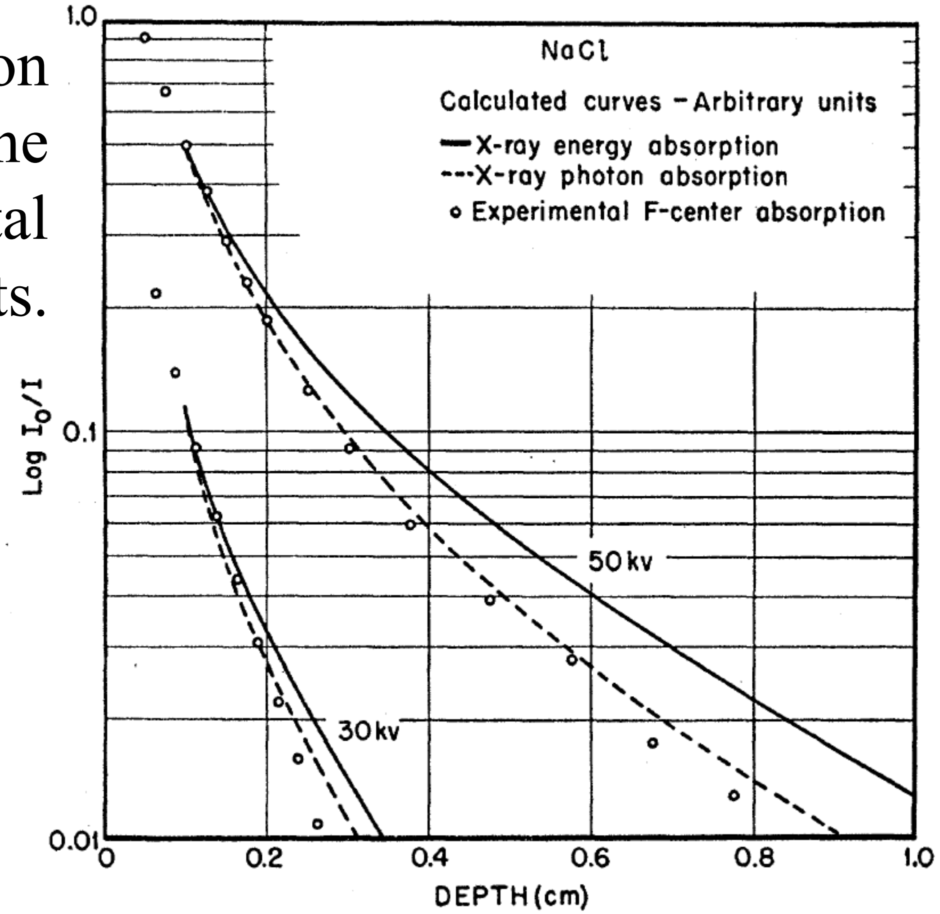

Dose Rate Information Is Enabled by Using Multiple Salts

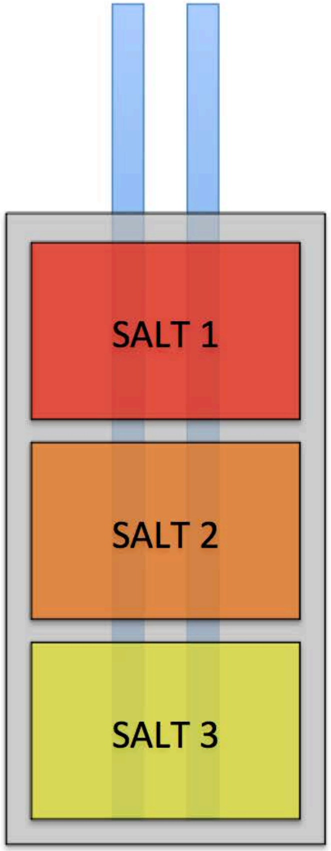

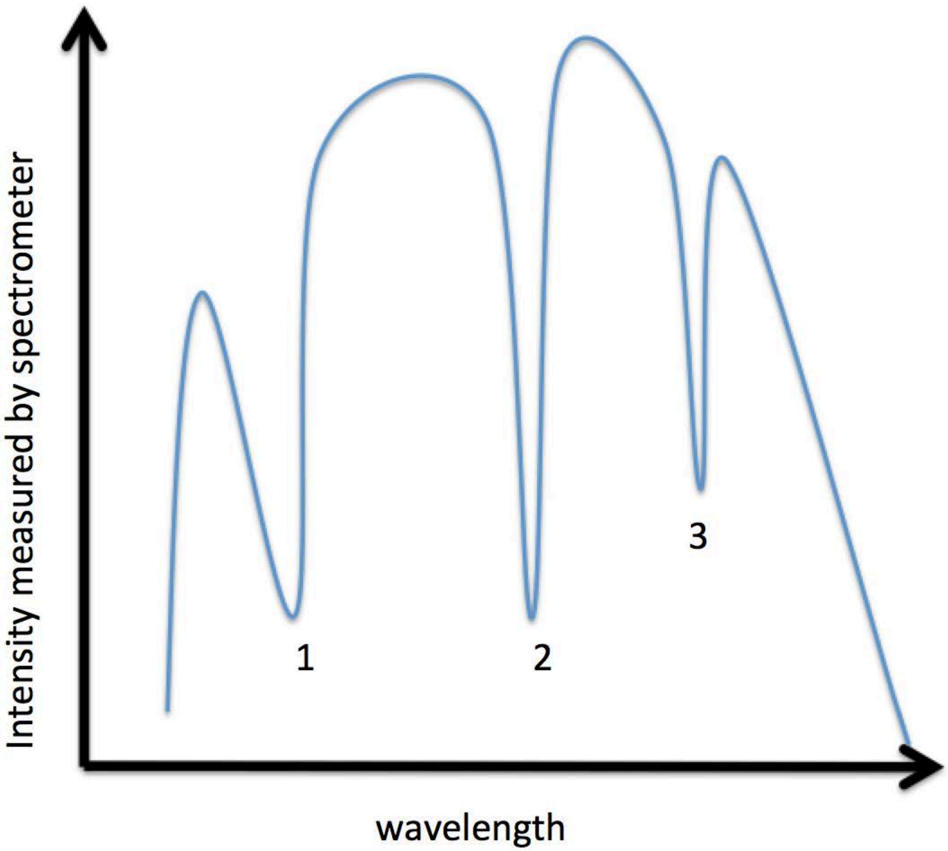

The IF^{2}D Remains Implanted during Fractional Treatments

- Avoids multiple insertion/removal surgeries
- Standard fiber optic port on patient allows optical connection in seconds

The IF^{2}D Feeds Back to the Proton Beam, Lowering Dose

Stops proton beam when IF^{2}D & tumor move out of beam range

Sends "ping" pulses to check whether the IF^{2}D and the tumor have returned

Turns proton beam on again when tumor is in beam range

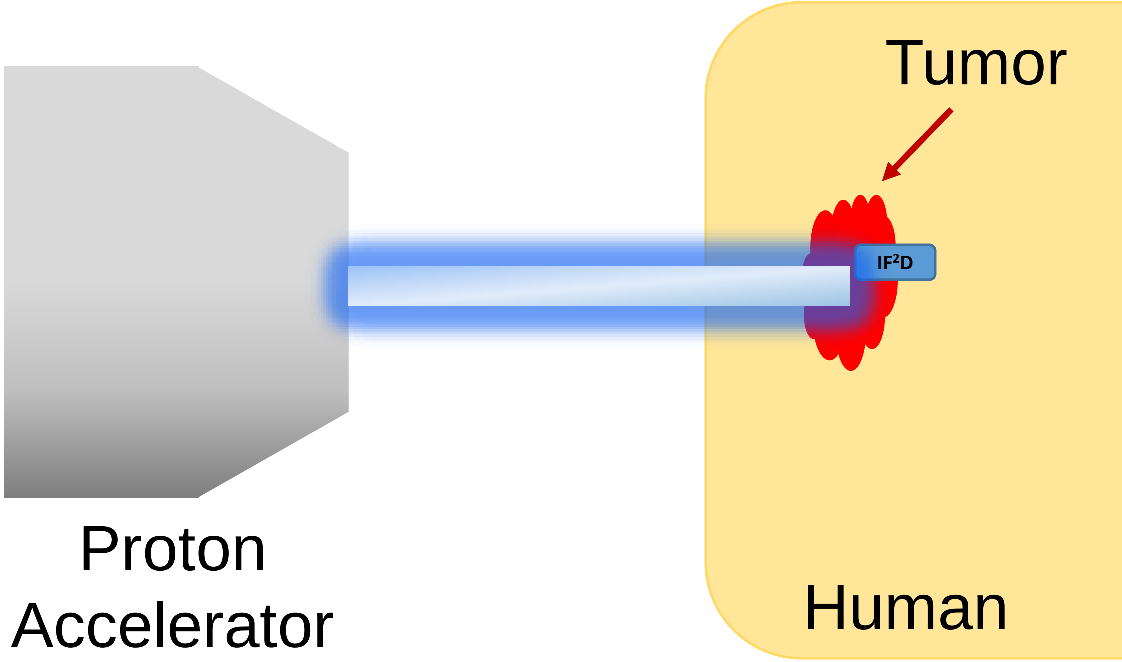

There Are Multiple IF^{2}D Implantation Options

- Multi-salt implant with fiber optic connection
- Single/dual wavelength absorber with LED light source
- All of the above on a chip, powered/read by RFID

What's Next in IF^{2}D Development

- Nail down dose vs. color changes (physics)
- Develop on-chip version (electrical)
- Find bio-compatible casing (medical)
- Secure initial seed funding or license IP (financial)
    - *Full patent & PCT filed, and received by the USPTO*

Increased Health Risks

From Turner, p. 458

Table 14.3 Probability Coefficients for Stochastic Effects (per Sv effective dose)

Detriment	Adult Workers (10^{-2} Sv^{-1})	Whole Population (10^{-2} Sv^{-1})
Fatal cancer	4.0	5.0
Nonfatal cancer	0.8	1.0
Severe genetic effects	0.8	1.3
Total	5.6	7.3

Source: ICRP Publication 60 and NCRP Report No. 116.

How Much Is Too Much?

From Turner, p. 459

The following recommendation is made by the NCRP for lifetime occupational exposure to radiation:

> The Council . . . recommends that the numerical value of the individual worker's lifetime effective dose in tens of mSv be limited to the value of his or her age in years (not including medical and natural background exposure).

To control the distribution of exposure over a working career,

> The Council recommends that the annual occupational effective dose be limited to 50 mSv (not including medical and background exposure).

How Much Is Too Much?

From Turner, p. 460

The NCRP makes the following recommendations for the exposure of an individual to man-made sources (natural background and medical exposures are not to be included):

> For continuous (or frequent) exposure, it is recommended that the annual effective dose not exceed 1 mSv . . . Furthermore, a maximum annual effective dose limit of 5 mSv is recommended to provide for infrequent annual exposures. . . .

How Much Is Enough?

From Turner, p. 461

Table 14.4 Exposure Limits from NCRP Report No. 116 and ICRP Publication 60

	NCRP-116	ICRP-60
Occupational Exposure		
Effective Dose		
Annual	50 mSv	50 mSv
Cumulative	10 mSv × age (y)	100 mSv in 5 y
Equivalent Dose		
Annual	150 mSv lens of eye; 500 mSv skin, hands, feet	150 mSv lens of eye; 500 mSv skin, hands, feet
Exposure of Public		
Effective Dose		
Annual	1 mSv if continuous 5 mSv if infrequent	1 mSv; higher if needed, provided 5-y annual average $\leqslant$1 mSv
Equivalent Dose		
Annual	15 mSv lens of eye; 50 mSv skin, hands, feet	15 mSv lens of eye; 50 mSv skin, hands, feet

How Much Is "Nothing?"

NCRP Report No. 116 defines a negligible individual dose (NID), without a corresponding risk level, as follows:

> The Council . . . recommends that an annual effective dose of 0.01 mSv be considered a Negligible Individual Dose (NID) per source or practice.

ICRP Publication 60 does not make a recommendation on the subject.

Normal Background Levels

https://radwatch.berkeley.edu/rad101

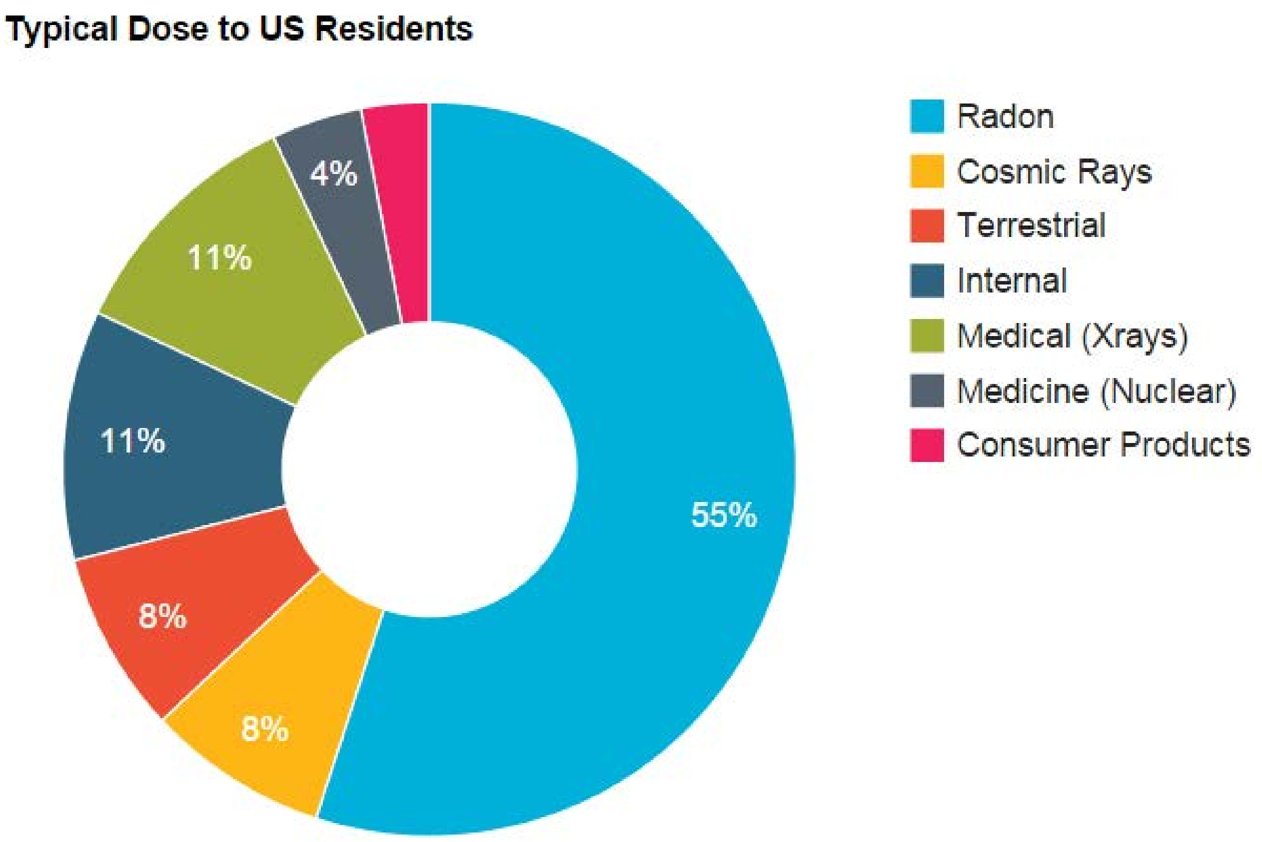

Image by Ryan Pavlovsky. Courtesy of Berkely RadWatch. Used with permission.

Natural Sources – Radon

http://www.nist.gov/pml/general/curie/1927.cfm

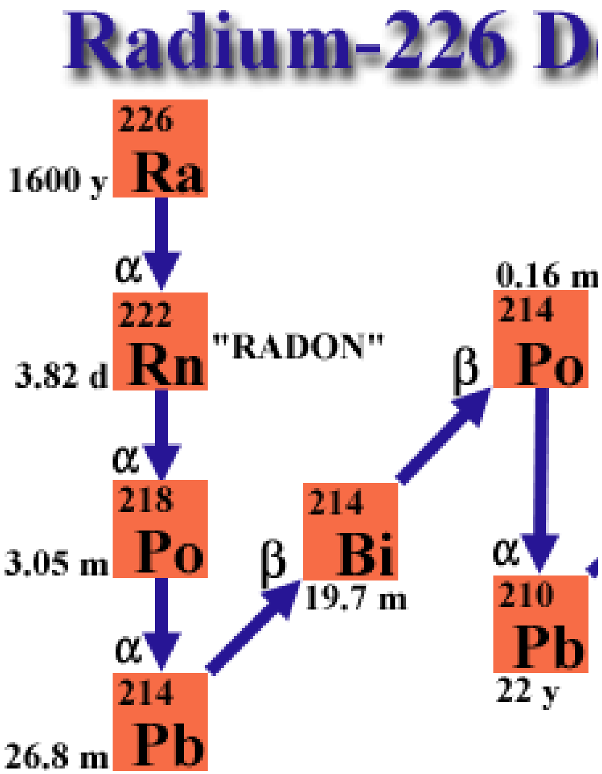

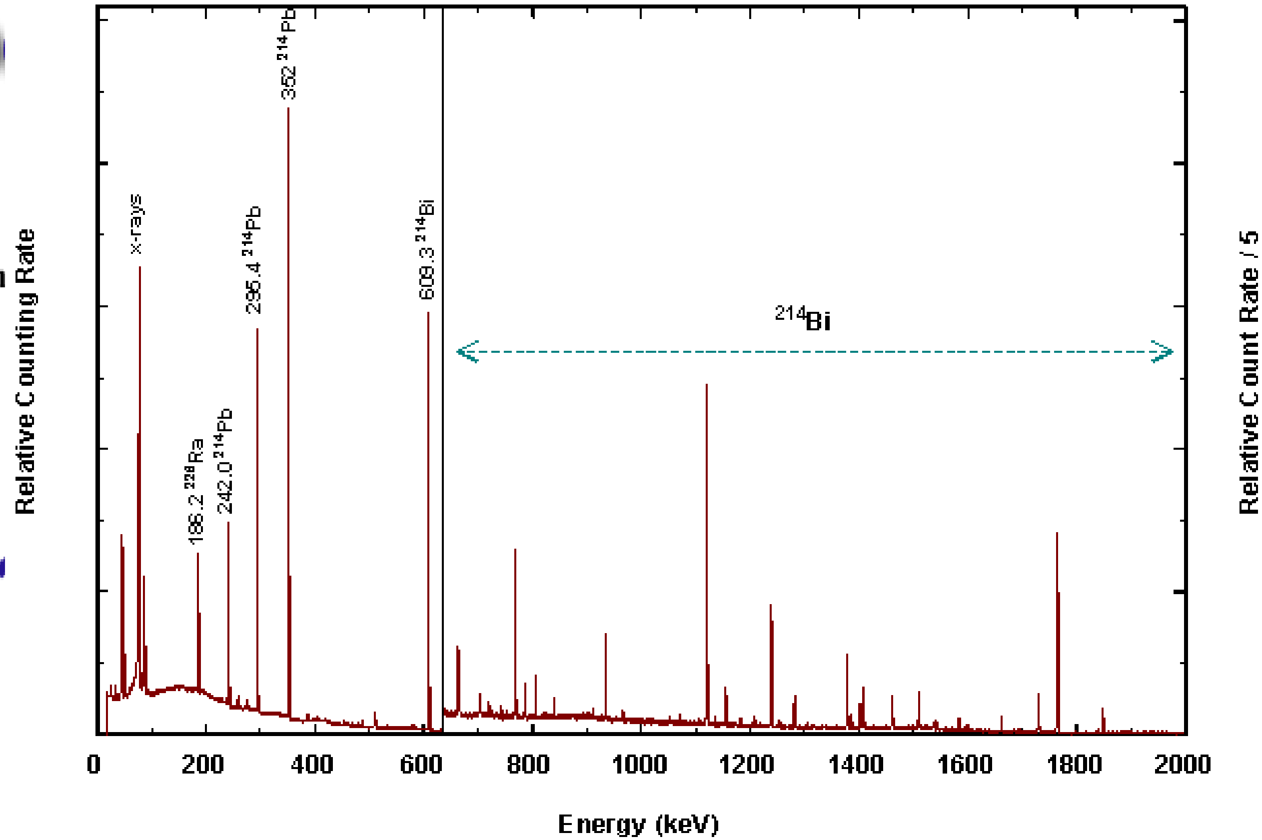

Images courtesy of U.S. DOC.

Radon Map of the U.S.

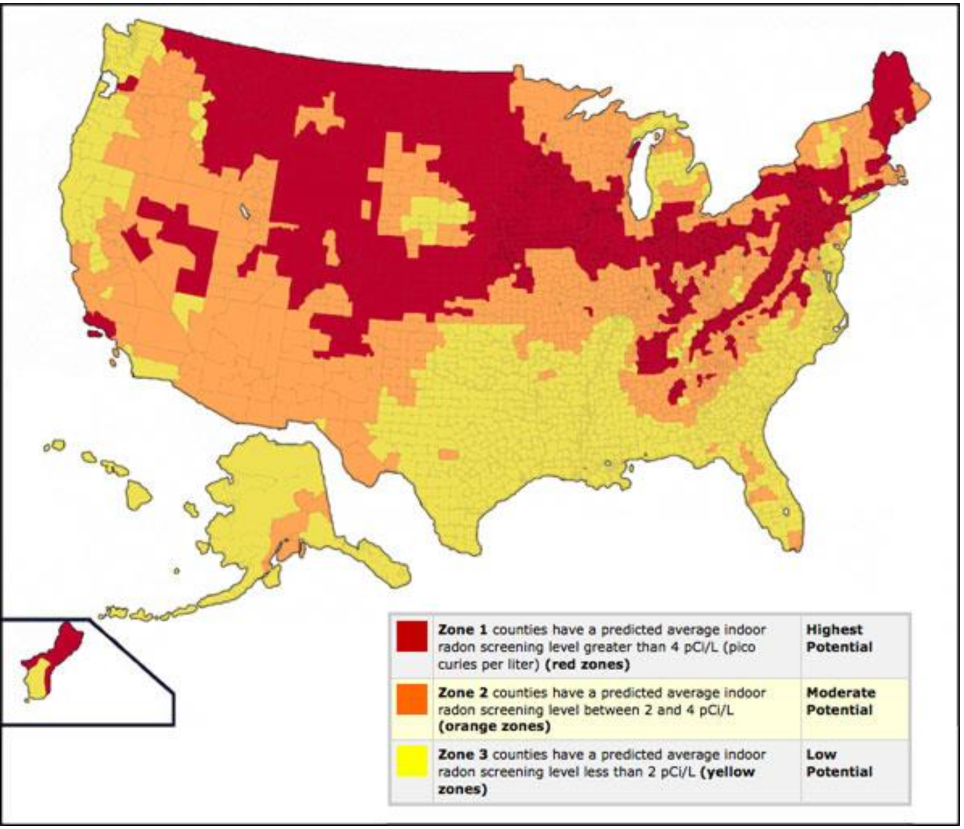

Public domain image, from U.S. EPA.

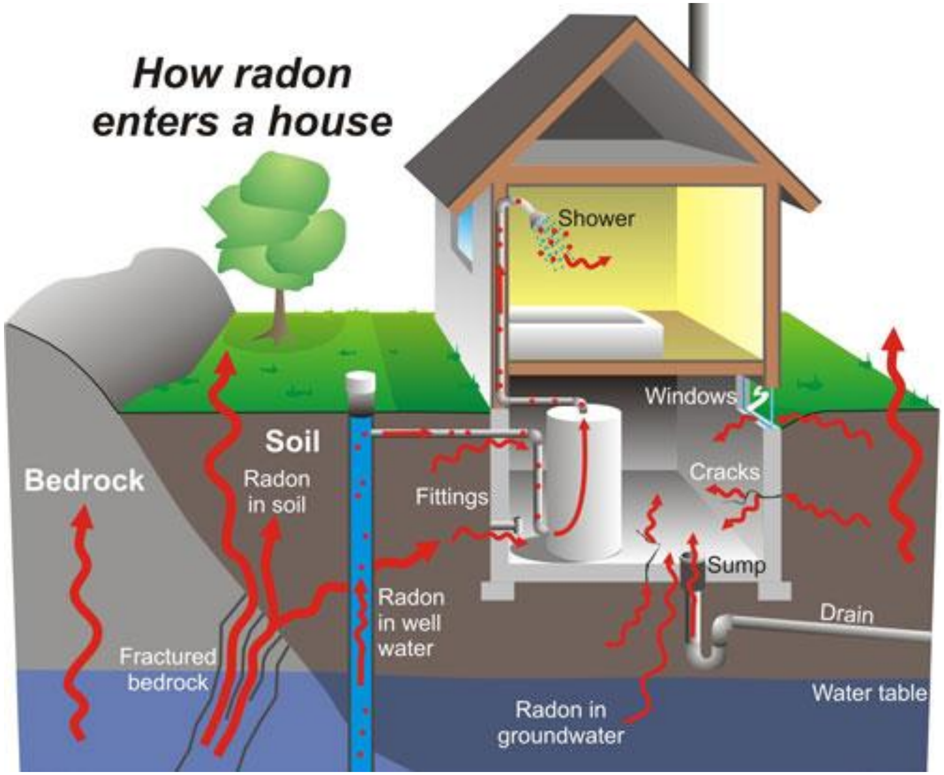

Relative Radon Risk

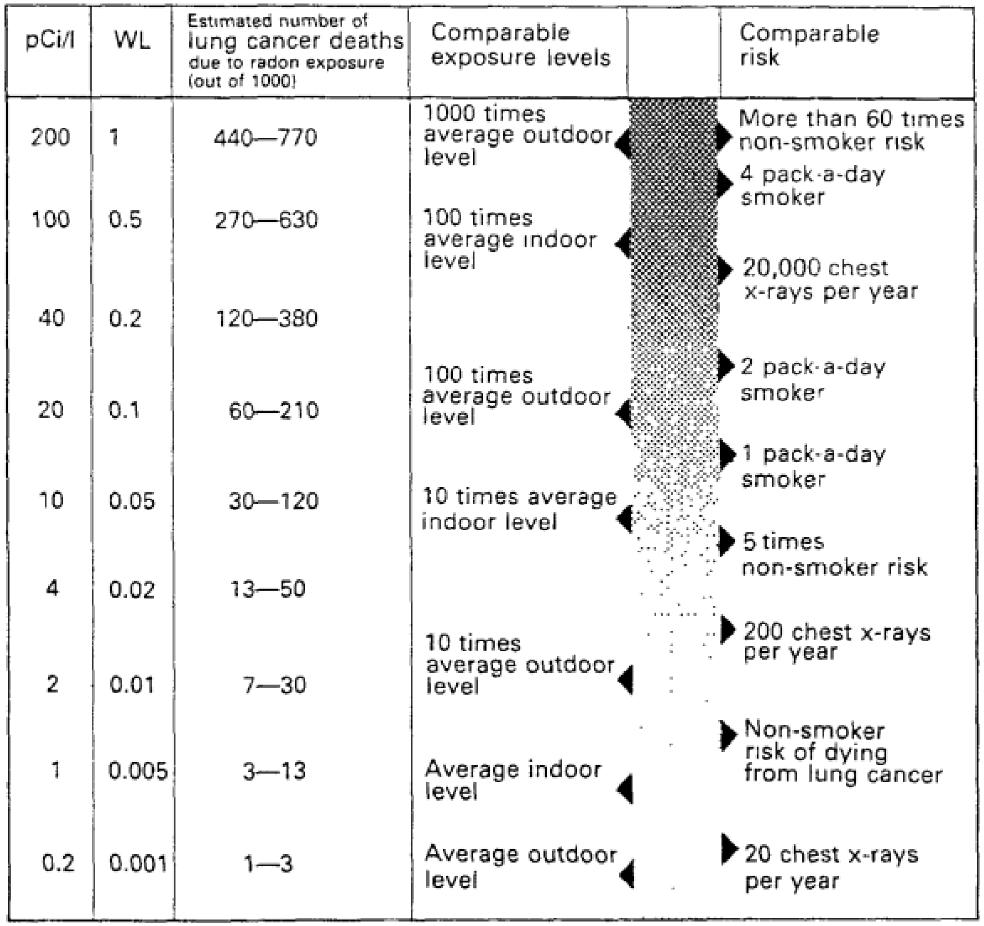

Radon Risk Evaluation Chart

pCi/l	WL	Estimated number of lung cancer deaths due to radon exposure (out of 1000)	Comparable exposure levels	Comparable risk
200	1	440—770	1000 times average outdoor level	More than 60 times non-smoker risk 4 pack-a-day smoker
100	0.5	270—630	100 times average indoor level	20,000 chest x-rays per year
40	0.2	120—380		
20	0.1	60—210	100 times average outdoor level	2 pack-a-day smoker
10	0.05	30—120	10 times average indoor level	1 pack-a-day smoker
4	0.02	13—50		5 times non-smoker risk
2	0.01	7—30	10 times average outdoor level	200 chest x-rays per year
1	0.005	3—13	Average indoor level	Non-smoker risk of dying from lung cancer
0.2	0.001	1—3	Average outdoor level	20 chest x-rays per year

Public domain image.

From EPA Publication OPA-86-004: “A Citizen’s Guide to Radon: What It Is and What To Do About It.” August 1986.

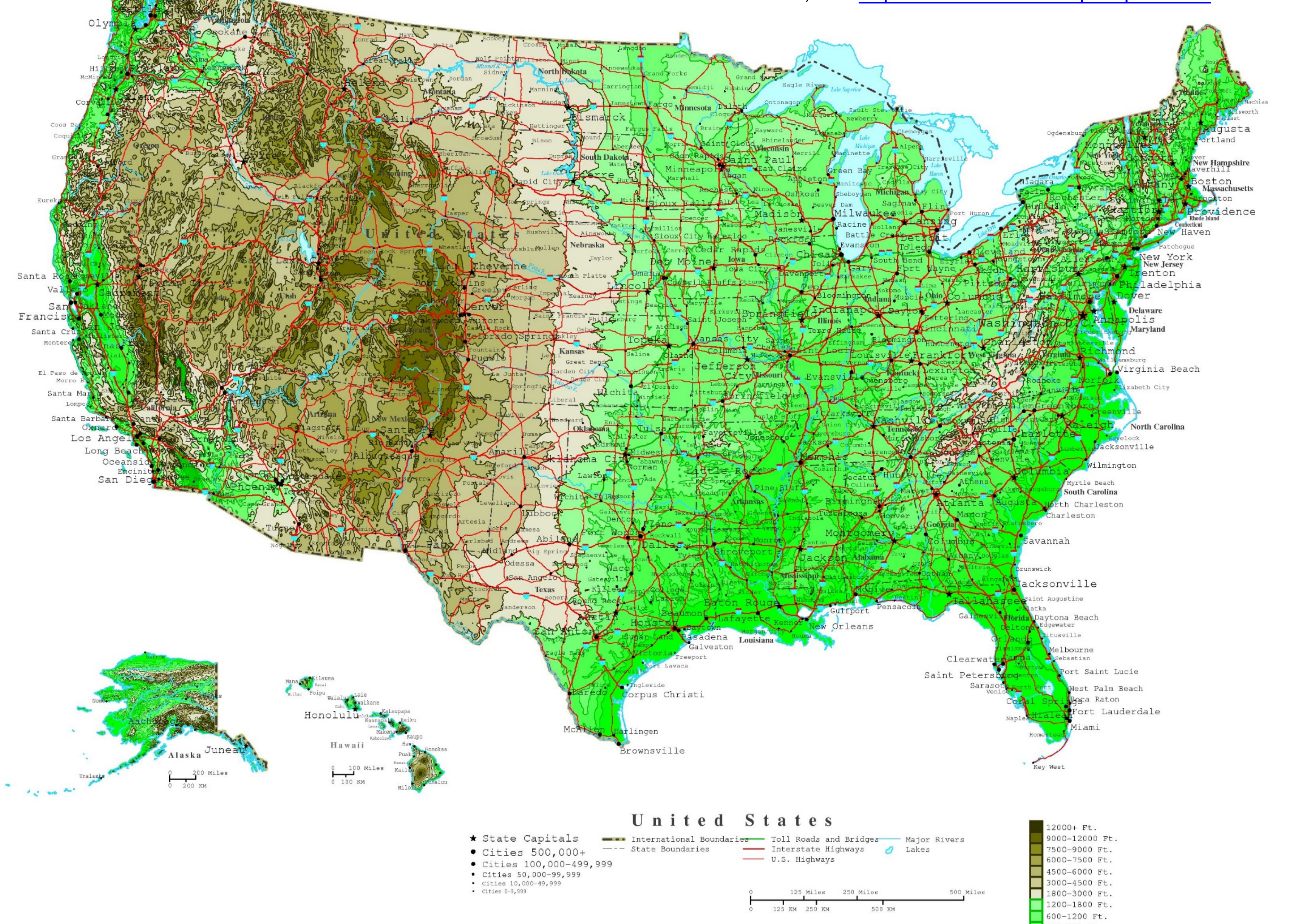
United States
State Capitals
Cities 500,000+
Cities 100,000-499,999
Cities 50,000-99,999
Cities 10,000-49,999
Cities 0-9,999
International Boundaries
State Boundaries
Toll Roads and Bridges
Interstate Highways
U.S. Highways
Major Rivers
Lakes
0 125 Miles 250 Miles 500 Miles
0 125 KM 250 KM 500 KM
12000+ Ft.
9000-12000 Ft.
7500-9000 Ft.
6000-7500 Ft.
4500-6000 Ft.
3000-4500 Ft.
1800-3000 Ft.
1200-1800 Ft.
600-1200 Ft.
Alaska
Juneau
0 200 Miles
0 200 KM
Hawaii
Honolulu
0 100 Miles
0 100 KM
Olympia
Spokane
Bismarck
Pierre
Duluth
Saint Paul
Minneapolis
Madison
Milwaukee
Chicago
Detroit
Lansing
Augusta
Portland
Boston
Providence
New Haven
New York
Trenton
Philadelphia
Dover
Annapolis
Washington D.C.
Richmond
Virginia Beach
Norfolk
Raleigh
Charlotte
Columbia
Wilmington
Savannah
Jacksonville
Tallahassee
Atlanta
Montgomery
Birmingham
Jackson
Nashville
Louisville
Frankfort
Indianapolis
Columbus
Cincinnati
Springfield
Saint Louis
Jefferson City
Kansas City
Topeka
Lincoln
Omaha
Des Moines
Wichita
Tulsa
Oklahoma City
Little Rock
Memphis
Shreveport
Dallas
Fort Worth
Austin
San Antonio
Houston
Baton Rouge
New Orleans
Corpus Christi
Laredo
Brownsville
Harlingen
McAllen
El Paso
Lubbock
Amarillo
Albuquerque
Santa Fe
Denver
Cheyenne
Colorado Springs
Pueblo
Phoenix
Tucson
Salt Lake
Boise
Sacramento
San Francisco
Santa Cruz
Los Angeles
Long Beach
Oceanside
San Diego
Miami
Fort Lauderdale
Boca Raton
West Palm Beach
Port Saint Lucie
Melbourne
Orlando
Daytona Beach
Tampa
Clearwater
Saint Petersburg
Key West
Gulfport
Pensacola
Galveston
Pasadena
Beaumont
Lafayette
Texas
Louisiana
North Carolina
South Carolina
New Hampshire
Massachusetts
Connecticut
Rhode Island
New Jersey
Delaware
Maryland
Nebraska
Kansas
Oklahoma
Iowa
Illinois
Minnesota
North Dakota
South Dakota
Montana
Wyoming
Lake Superior
Lake Michigan
Lake Huron

The Primordial Nuclides

Shultis, J. K., and R. E. Faw. *Fundamentals of Nuclear Science and Engineering*, 2nd Edition. CRC Press, 2007.

Table 5.2. The 17 isolated primordial radionuclides. Data taken from GE-NE [1996].

Radionuclide	& the Decay Modes	Half-life (years)	% El. Abund.	Radionuclide	& the Decay Modes	Half-life (years)	% El. Abund.
$^{40}_{19}K$	β^- EC β^+	1.27×10^{9}	0.0117	$^{50}_{23}V$	β^- EC	1.4×10^{17}	0.250
$^{87}_{37}Rb$	β^-	4.88×10^{10}	27.84	$^{113}_{48}Cd$	β^-	9×10^{15}	12.22
$^{115}_{49}In$	β^-	4.4×10^{14}	95.71	$^{123}_{52}Te$	EC	$> 1.3 \times 10^{13}$	0.908
$^{138}_{57}La$	EC β^-	1.05×10^{11}	0.090	$^{144}_{60}Nd$	α	2.38×10^{15}	23.80
$^{147}_{62}Sm$	α	1.06×10^{11}	15.0	$^{148}_{62}Sm$	α	7×10^{15}	11.3
$^{152}_{64}Gd$	α	1.1×10^{14}	0.20	$^{176}_{71}Lu$	β^-	3.78×10^{10}	2.59
$^{174}_{72}Hf$	α	2.0×10^{15}	0.162	$^{180}_{73}Ta$	EC β^+	$> 1.2 \times 10^{15}$	0.012
$^{187}_{75}Re$	β^-	4.3×10^{10}	62.60	$^{186}_{76}Os$	α	2×10^{15}	1.58
$^{190}_{78}Pt$	α	6.5×10^{11}	0.01				

Nuclides in Building Materials

Data from http://www.physics.isu.edu/radinf/natural.htm

(NCRP 94, 1987, except where noted)						
Material	Uranium		Thorium		Potassium	
	ppm	mBq/g (pCi/g)	ppm	mBq/g (pCi/g)	ppm	mBq/g (pCi/g)
Granite	4.7	63 (1.7)	2	8 (0.22)	4.0	1184 (32)
Sandstone	0.45	6 (0.2)	1.7	7 (0.19)	1.4	414 (11.2)
Cement	3.4	46 (1.2)	5.1	21 (0.57)	0.8	237 (6.4)
Limestone concrete	2.3	31 (0.8)	2.1	8.5 (0.23)	0.3	89 (2.4)
Sandstone concrete	0.8	11 (0.3)	2.1	8.5 (0.23)	1.3	385 (10.4)
Dry wallboard	1.0	14 (0.4)	3	12 (0.32)	0.3	89 (2.4)
By-product gypsum	13.7	186 (5.0)	16.1	66 (1.78)	0.02	5.9 (0.2)
Natural gypsum	1.1	15 (0.4)	1.8	7.4 (0.2)	0.5	148 (4)
Wood	-	-	-	-	11.3	3330 (90)
Clay Brick	8.2	111 (3)	10.8	44 (1.2)	2.3	666 (18)

Nuclides in Seawater

Data from http://www.physics.isu.edu/radinf/natural.htm

Nuclide	Activity used in calculation	Activity in Ocean		
		Pacific	Atlantic	All Oceans
Uranium	0.9 pCi/L (33 mBq/L)	6×10^{8} Ci (22 EBq)	3×10^{8} Ci (11 EBq)	1.1×10^{9} Ci (41 EBq)
Potassium 40	300 pCi/L (11 Bq/L)	2×10^{11} Ci (7400 EBq)	9×10^{10} Ci (3300 EBq)	3.8×10^{11} Ci (14000 EBq)
Tritium	0.016 pCi/L (0.6 mBq/L)	1×10^{7} Ci (370 PBq)	5×10^{6} Ci (190 PBq)	2×10^{7} Ci (740 PBq)
Carbon 14	0.135 pCi/L (5 mBq/L)	8×10^{7} Ci (3 EBq)	4×10^{7} Ci (1.5 EBq)	1.8×10^{8} Ci (6.7 EBq)
Rubidium 87	28 pCi/L (1.1 Bq/L)	1.9×10^{10} Ci (700 EBq)	9×10^{9} Ci (330 EBq)	3.6×10^{10}

Uranium from Seawater?

http://nextbigfuture.com/2007_11_04_archive.html

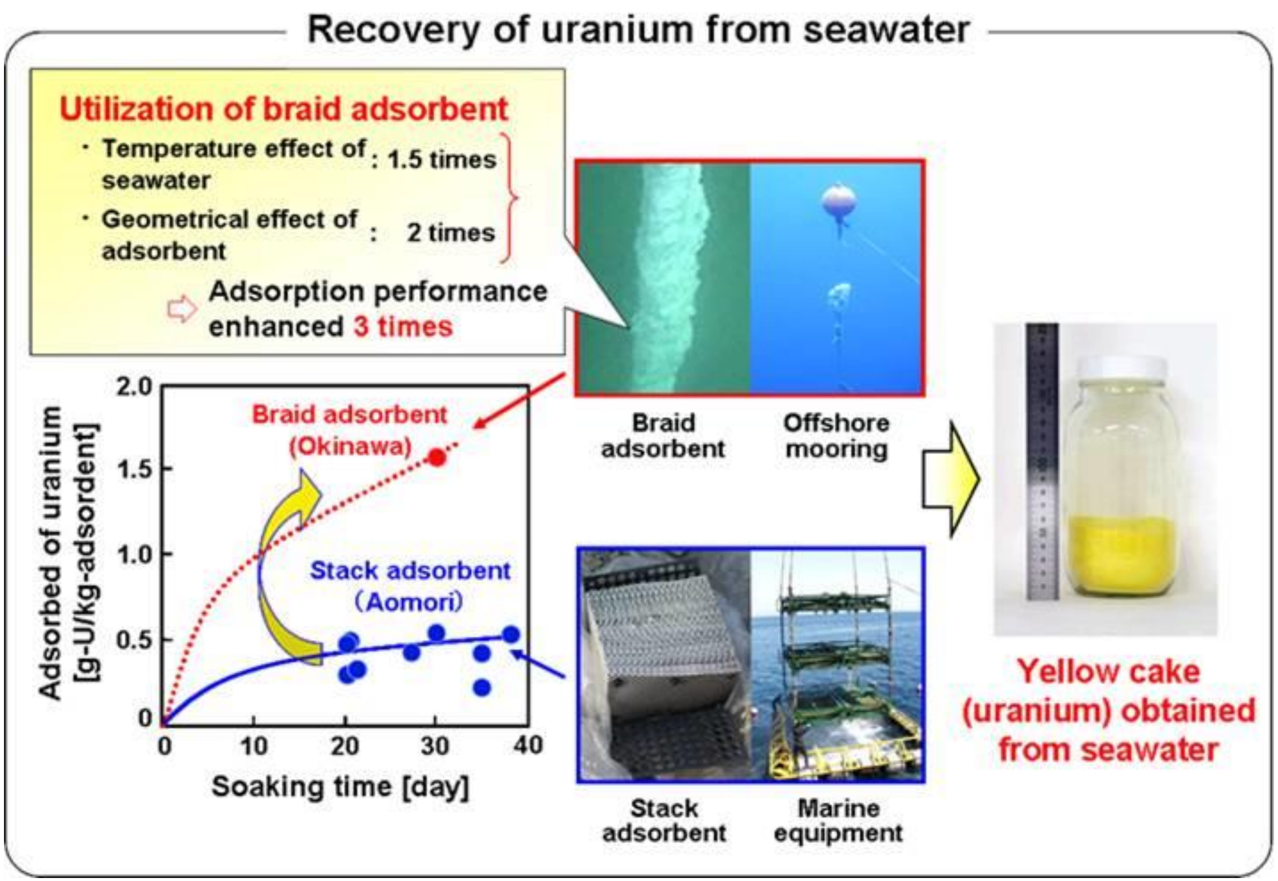

Uranium from Seawater!

Chemical Science RSC Publishing

EDGE ARTICLE

View Article Online
View Journal | View Issue

Highly porous and stable metal–organic frameworks for uranium extraction†

Cite this: *Chem. Sci.*, 2013, **4**, 2396

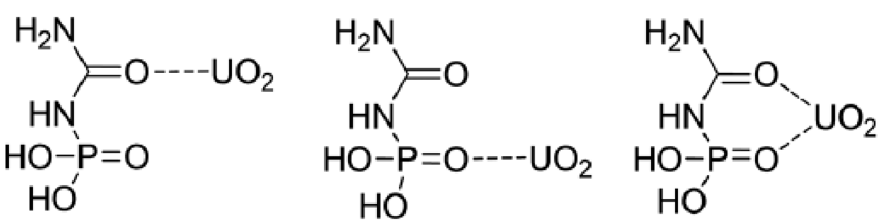

I **II** **III**

Fig. 6 Three uranyl binding motifs for carbamoylphosphoramidic acid investigated by DFT calculations: uranyl bound to carbonyl oxygen (**I**), uranyl bound to phosphoryl oxygen (**II**), and bidentate uranyl coordination (**III**).

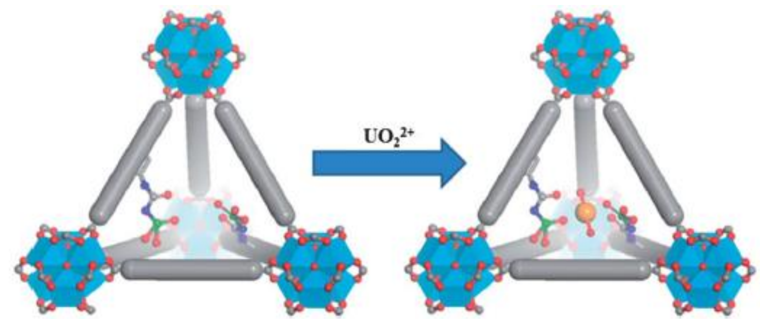

ig. 9 Simplified schematic depicting the uranyl-binding pocket formed in the etrahedron of the MOFs. UO_2^{2+} is coordinated in a monodentate fashion to the hosphoryl oxygen. Distances between oxygen range from 4.5–4.8 Å, accommodating U–O bond lengths appropriate for binding motif **II–II**.

Radioactivity in the Body

Data from http://www.physics.isu.edu/radinf/natural.htm

Nuclide	Total Mass of Nuclide Found in the Body	Total Activity of Nuclide Found in the Body	Daily Intake of Nuclides
Uranium	90 µg	30 pCi (1.1 Bq)	1.9 µg
Thorium	30 µg	3 pCi (0.11 Bq)	3 µg
Potassium 40	17 mg	120 nCi (4.4 kBq)	0.39 mg
Radium	31 pg	30 pCi (1.1 Bq)	2.3 pg
Carbon 14	22 ng	0.1 µCi (3.7 kBq)	1.8 ng
Tritium	0.06 pg	0.6 nCi (23 Bq)	0.003 pg
Polonium	0.2 pg	1 nCi (37 Bq)	~0.6 f

Medical Procedures

Typical Effective Radiation Dose from Diagnostic X Ray—Single Exposure (Mettler 2008)

Mettler FA Jr, et al. *Radiology* 248(1):254-263; 2008.

Exam	Effective Dose mSv (mrem)
Chest	0.1 (10)
Cervical Spine	0.2 (20)
Thoracic Spine	1.0 (100)
Lumbar Spine	1.5 (150)
Pelvis	0.7 (70)
Abdomen or Hip	0.6 (60)
Mammogram (2 view)	0.36 (36)
Dental Bitewing	0.005 (0.5)
Dental (panoramic)	0.01 (1)
DEXA (whole body)	0.001 (0.1)
Skull	0.1 (10)
Hand or Foot	0.005 (0.5)

Examinations and Procedures	Effective Dose mSv (mrem)
Intravenous Pyelogram	3.0 (300)
Upper GI	6.0 (600)
Barium Enema	7.0 (700)
Abdomen Kidney, Ureter, Bladder (KUB)	0.7 (70)
CT Head	2.0 (200)
CT Chest	7.0 (700)
CT Abdomen/Pelvis	10.0 (1,000)
Whole-Body CT Screening	10.0 (1,000)
CT Biopsy	1.0 (100)
Calcium Scoring	2.0 (200)
Coronary Angiography	20.0 (2,000)
Cardiac Diagnostic & Intervention	30.0 (3,000)
Pacemaker Placement	1.0 (100)
Peripheral Vascular Angioplasties	5.0 (500)
Noncardiac Embolization	55.0 (5,500)
Vertebroplasty	16.0 (1,600)

More Medical Procedures

Mettler FA Jr, et al. *Radiology* 248(1):254-263; 2008.

Typical Effective Radiation Dose from Nuclear Medicine Examinations (Mettler 2008)

Nuclear Medicine Scan Radiopharmaceutical (common trade name)	Effective Dose mSv (mrem)
Brain (PET) ^{18}F FDG	14.1 (1,410)
Brain (perfusion) ^{99m}Tc HMPAO	6.9 (690)
Hepatobiliary (liver flow) ^{99m}Tc Sulfur Colloid	2.1 (210)
Bone ^{99m}Tc MDP	6.3 (630)
Lung Perfusion/Ventilation ^{99m}Tc MAA & ^{133}Xe	2.5 (250)
Kidney (filtration rate) ^{99m}Tc DTPA	1.8 (180)
Kidney (tubular function) ^{99m}Tc MAG3	2.2 (220)
Tumor/Infection ^{67}Ga	2.5 (250)
Heart (stress-rest) ^{99m}Tc sestamibi (Cardiolite)	9.4 (940)
Heart (stress-rest) ^{201}Tl chloride	41.0 (4,100)
Heart (stress-rest) ^{99m}Tc tetrofosmin (Myoview)	11.0 (1,100)
Various PET Studies ^{18}F FDG	14.0 (1,400)

Radiation from Altitude

http://www.ansto.gov.au/NuclearFacts/Whatisradiation/

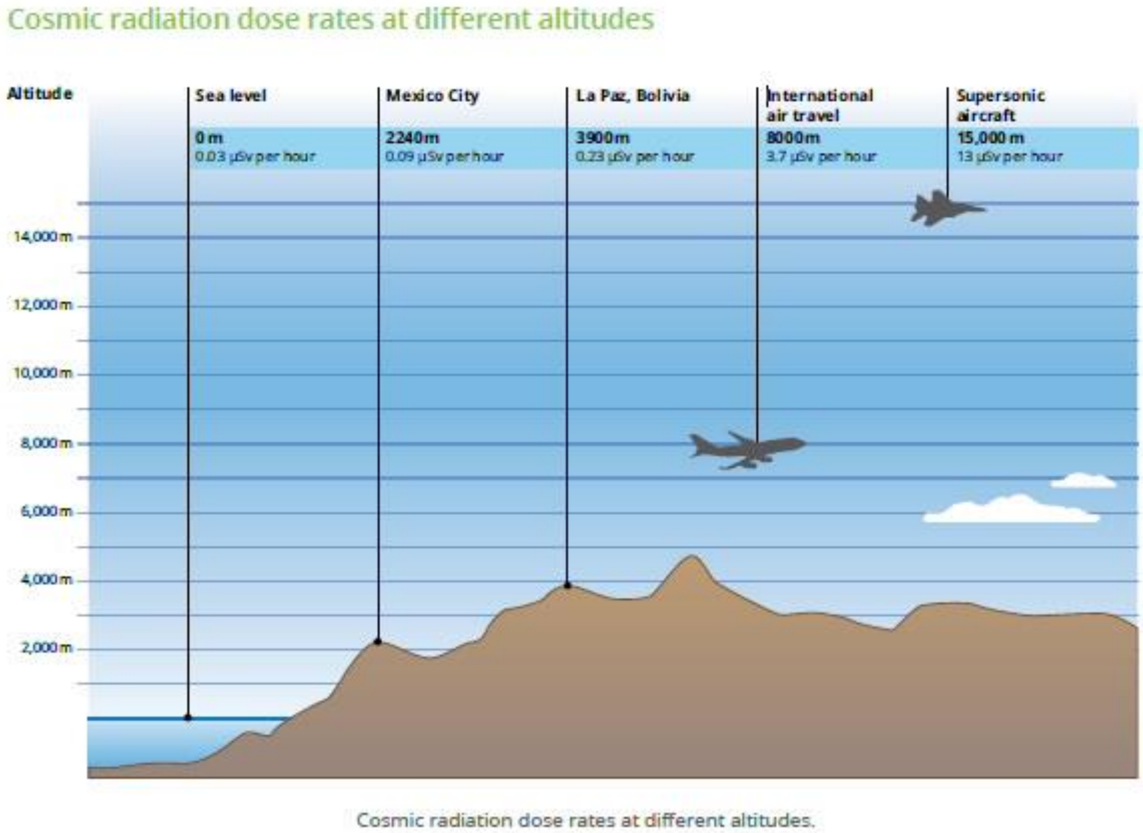

Cosmic radiation dose rates at different altitudes.

Radiation from Flying

http://www.spaceweather.com – Nov. 16, 2014

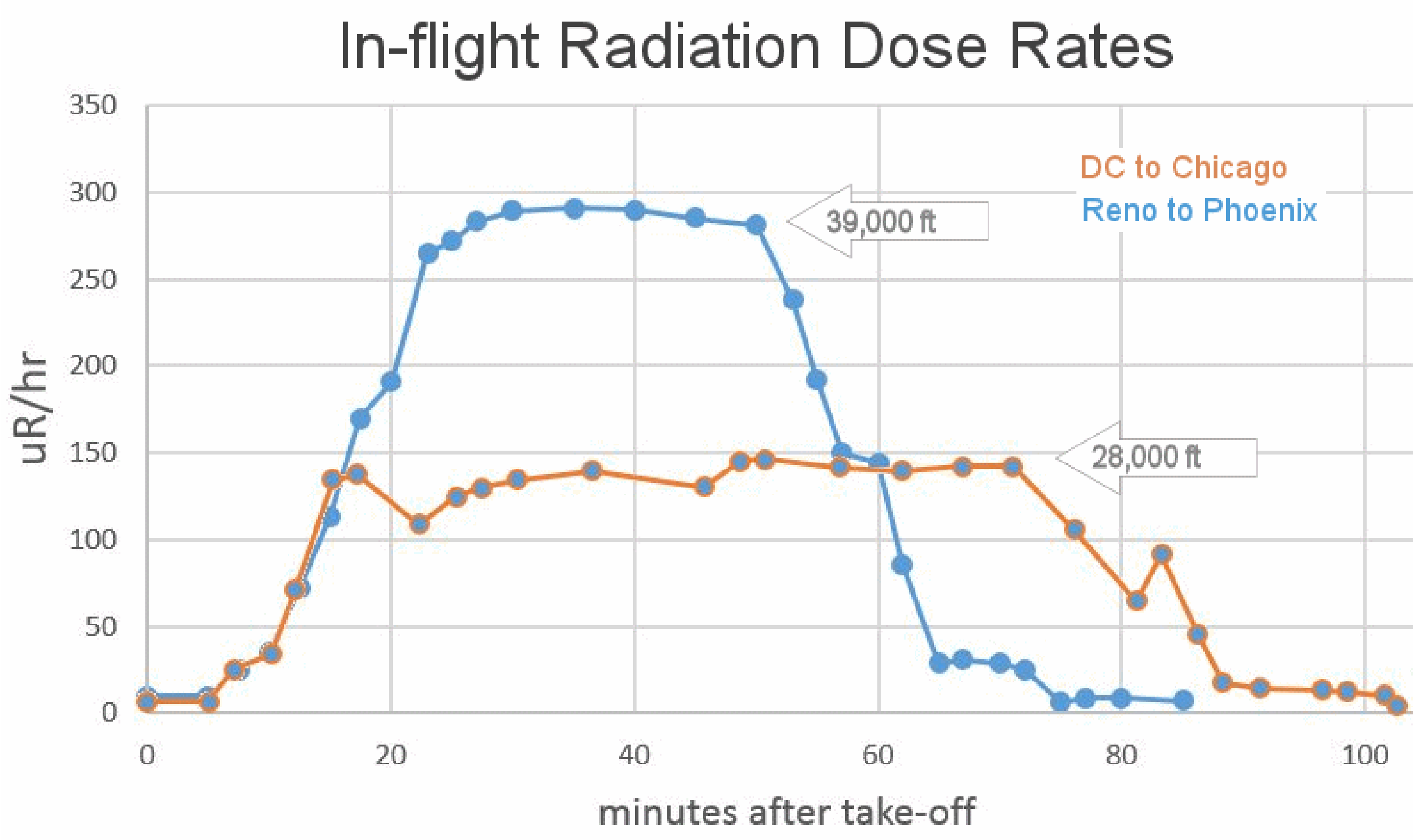

Courtesy of Spaceweather.com. Used with permission.

Cosmic Rays – Origin

http://photojournal.jpl.nasa.gov/jpeg/PIA16938.jpg

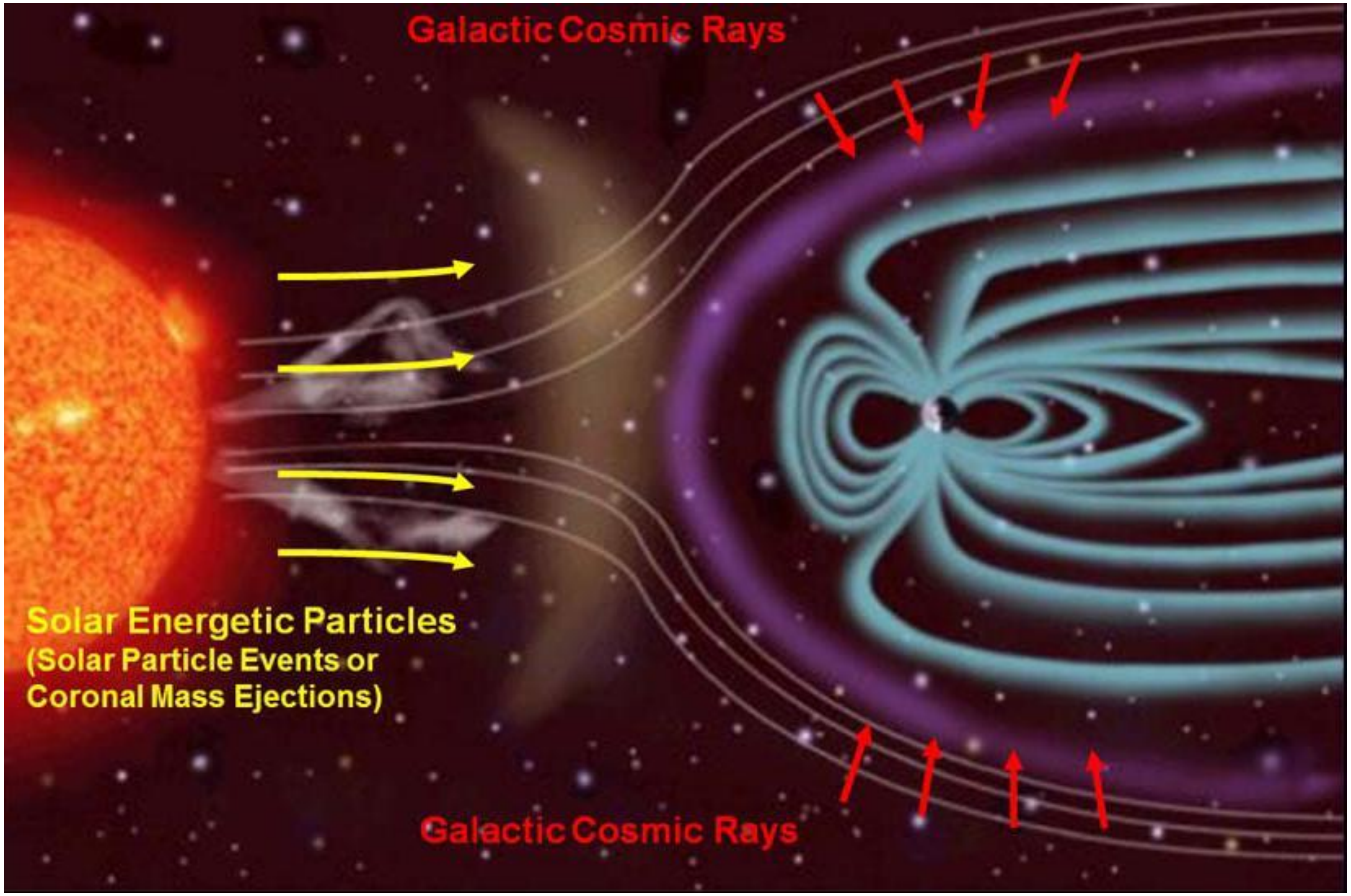

Solar Cosmic Ions – Origin

Klein, K-L., and G. Trottet. ***Space Science Reviews*** **95: 215–225, 2001**

<u>Abstract</u>

We review evidence that led to the view that acceleration at shock waves driven by coronal mass ejections (CMEs) is responsible for large particle events detected at 1 AU. It appears that even if the CME bow shock acceleration is a possible model for the origin of rather low energy ions, it faces difficulties on account of the production of ions far above 1 MeV: (i) although shock waves have been demonstrated to accelerate ions to energies of some MeV nucl^{-1} in the interplanetary medium, their ability to achieve relativistic energies in the solar environment is unproven; (ii) SEP events producing particle enhancements at energies 100 MeV are also accompanied by flares; those accompanied only by fast CMEs have no proton signatures above 50 MeV. We emphasize detailed studies of individual high energy particle events which provide strong evidence that **time-extended particle acceleration which occurs in the corona after the impulsive flare contributes to particle fluxes in space. It appears thus that the CME bow shock scenario has been overvalued and that long lasting coronal energy release processes have to be taken into account when searching for the origin of high energy SEP events.**

Making Cosmogenic Nuclides

- Protons enter the atmosphere
- ***Spallation*** occurs, releasing neutrons
- Neutrons combine with key nuclides to produce ^{3}H, ^{14}C
  - $^{14}N(n,p)^{14}C$
  - $^{14}N(n,^{3}H)^{12}C$

Spallation Sources on Earth

http://pd.chem.ucl.ac.uk/pdnn/inst3/pulsed.htm

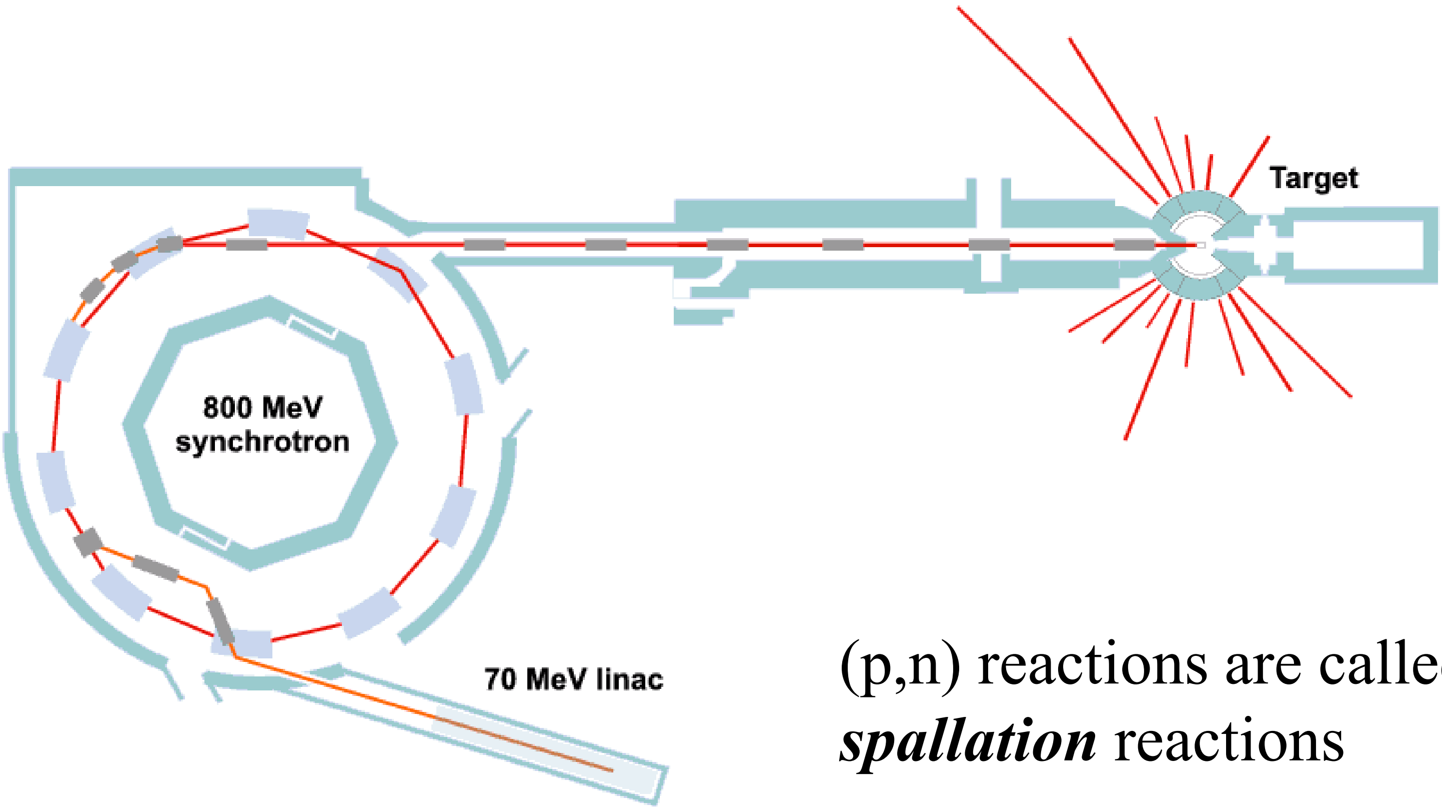

(p,n) reactions are called ***spallation*** reactions

Spallation on Earth – The SNS

http://neutrons2.ornl.gov/facilities/SNS/works.shtml

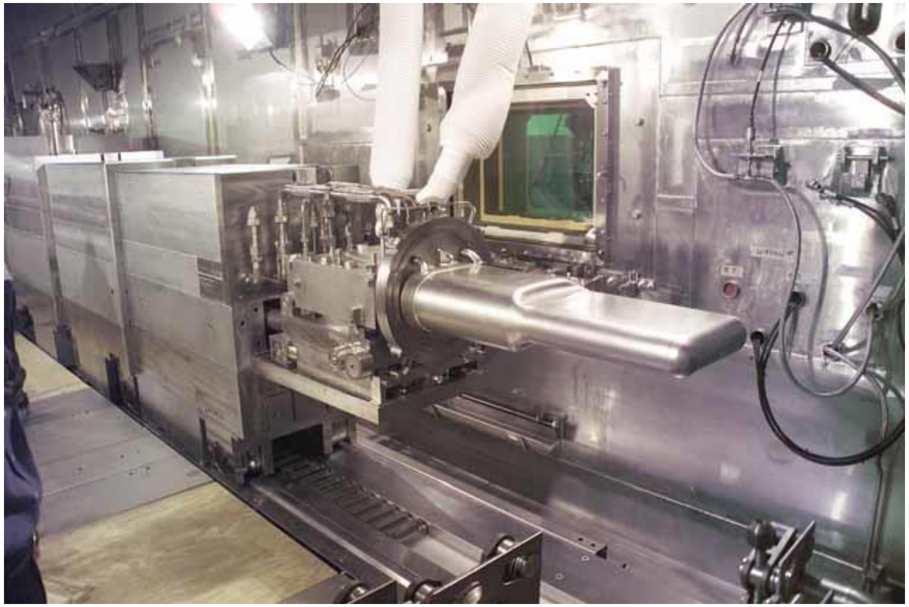

Courtesy of Oak Ridge National Laboratory, U.S. Dept. of Energy.

Nuclear Craziness from Electrons

http://chandra.harvard.edu/resources/illustrations/x-raysLight.html

Electrons can also create high-energy gamma rays by…

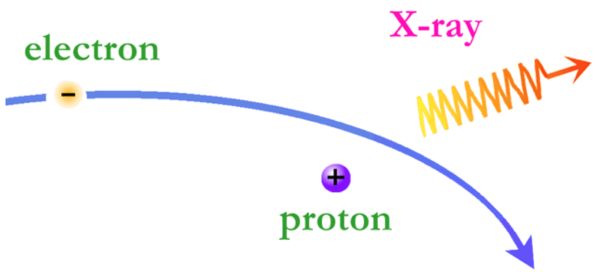

Bremsstrahlung

Synchrotron Radiation

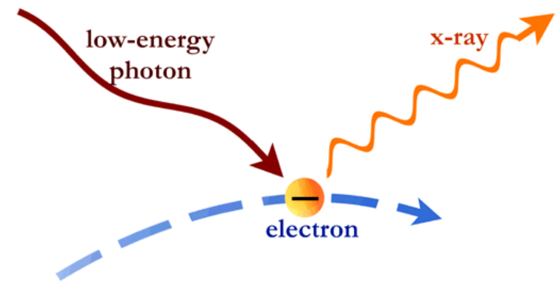

Inverse Compton Scattering

Inverse Compton Scattering

http://eud.gsfc.nasa.gov/Volker.Beckmann/school/download/Longair_Radiation3.pdf

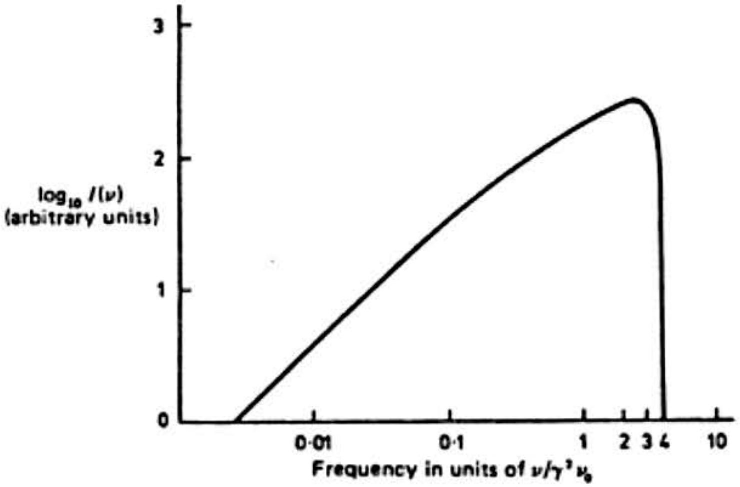

It is an easy calculation to show that the maximum energy which the photon can acquire corresponds to a head-on collision in which the photon is sent back along its original path. The maximum energy of the photon is

$$(\hbar\omega)_{\max} = \hbar\omega\gamma^2(1+v/c)^2 \approx 4\gamma^2\hbar\omega_0. \quad (14)$$

Another interesting result comes out of the formula for the total energy loss rate of the electron (11). The number of photons scattered per unit time is $\sigma_T c U_{\mathrm{rad}}/\hbar\omega_0$ and hence the average energy of the scattered photons is

$$\hbar\omega = \frac{4}{3}\gamma^2(v/c)^2\hbar\omega_0 \approx \frac{4}{3}\gamma^2\hbar\omega_0. \quad (15)$$

Identifying Radio Sources with Inverse Compton Scattering

http://eud.gsfc.nasa.gov/Volker.Beckmann/school/download/Longair_Radiation3.pdf

Cygnus A

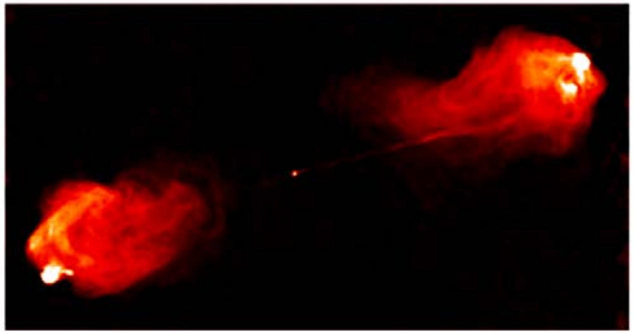

Radio Map from VLA

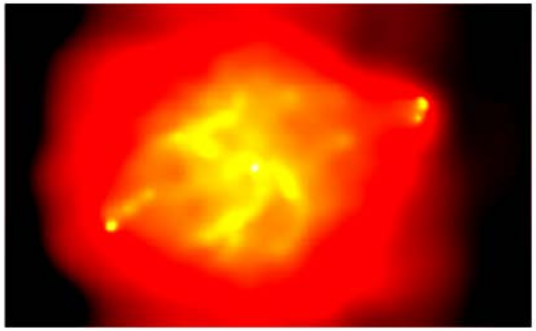

Chandra X-ray Map

Images courtesy of the National Radio Astronomy Observatory and NASA/UMD/A.Wilson et al.

The hot-spots of Cygnus A is a good example of this. According to Wilson, Young and Shopbell (2002), if the X-ray hot-spots are identified with inverse Compton scattering of the radio synchrotron emission within the lobes (Synchrotron-self Compton Radiation - see later), the magnetic field strength is 1.5×10^{-4} G. This figure is close to the equipartition value of the magnetic field strengths $2.5 - 2.8 \times 10^{-4}$ G, assuming $\eta = 0$. It is inferred that the relativistic plasma may well be an electron-positron plasma. Similar results are found in hot spots in other double radio sources.

What Happens to the Electrons?

http://eud.gsfc.nasa.gov/Volker.Beckmann/school/download/Longair_Radiation3.pdf

The Maximum Lifetimes of High Energy Electrons

An important piece of astrophysics involving the Cosmic Microwave Background Radiation is that relativistic electrons can never escape from it since it permeates all space. The energy density of the Cosmic Microwave Background Radiation is $U_0 = aT^4 = 2.6 \times 10^5$ eV m^{-3}. Therefore, the maximum lifetime τ of any electron against inverse Compton Scattering is

$$\tau = \frac{E}{|\mathrm{d}E/\mathrm{d}t|} = \frac{E}{\frac{4}{3}\sigma_\mathrm{T} c \gamma^2 U_0} = \frac{2.3 \times 10^{12}}{\gamma} \text{years} \qquad (19)$$

For example, we observe 100 GeV electrons at the top of the atmosphere and so they must have lifetimes $\tau \leq 10^7$ years.

Proton Collisions Create Pions

http://eud.gsfc.nasa.gov/Volker.Beckmann/school/download/Longair_Radiation3.pdf

γ-ray Processes and Photon-Photon Interactions

The processes of synchrotron radiation, inverse Compton scattering and relativistic bremsstrahlung are effective means of creating high-energy γ-ray photons, but there are other mechanisms. One of the most important is the decay of neutral pions created in collisions between relativistic protons and nuclei of atoms and ions of the interstellar gas.

$$\mathrm{p} + \mathrm{p} \rightarrow \pi^+, \pi^-, \pi^0. \tag{30}$$

The charged pions decay into muons and neutrinos

$$\pi^+ \rightarrow \mu^+ + \nu_\mu \quad ; \quad \pi^- \rightarrow \mu^- + \bar{\nu}_\mu \tag{31}$$

with a mean lifetime of 2.551×10^{-8} s. The charged muons then decay with mean lifetime of 2.2001×10^{-6} s

$$\mu^+ \rightarrow \mathrm{e}^+ + \nu_\mathrm{e} + \bar{\nu}_\mu \quad ; \quad \mu^- \rightarrow \mathrm{e}^- + \bar{\nu}_\mathrm{e} + \nu_\mu. \tag{32}$$

Neutral Pions Create Gammas

http://eud.gsfc.nasa.gov/Volker.Beckmann/school/download/Longair_Radiation3.pdf

In contrast, the neutral pions decay into pairs of γ-rays, $\pi^0 \rightarrow \gamma + \gamma$, in only 1.78×10^{-16} s. The cross-section for this process is $\sigma_{\mathrm{pp}\rightarrow\gamma\gamma} \approx 10^{-30}$ m^2 and the emitted spectrum of γ-rays has a broad maximum centred on a γ-ray energy of about 70 MeV (see *HEA2*, Sect. 20.1). This is the process responsible for the continuum emission of the interstellar gas at energies $\varepsilon \geq 100$ MeV. A simple calculation shows that, if the mean number density of the interstellar gas is $N \sim 10^6$ m^{-3} and the average energy density of cosmic ray protons with energies greater than 1 GeV about 10^6 eV m^{-3}, the γ-ray luminosity of the disc of our Galaxy is about 10^{32} W, as observed.

Pions – A Short Detour into Subatomic Physics

http://schoolphysics.co.uk/age16-19/Nuclear%20physics/Nuclear%20structure/text/Quarks_/index.html

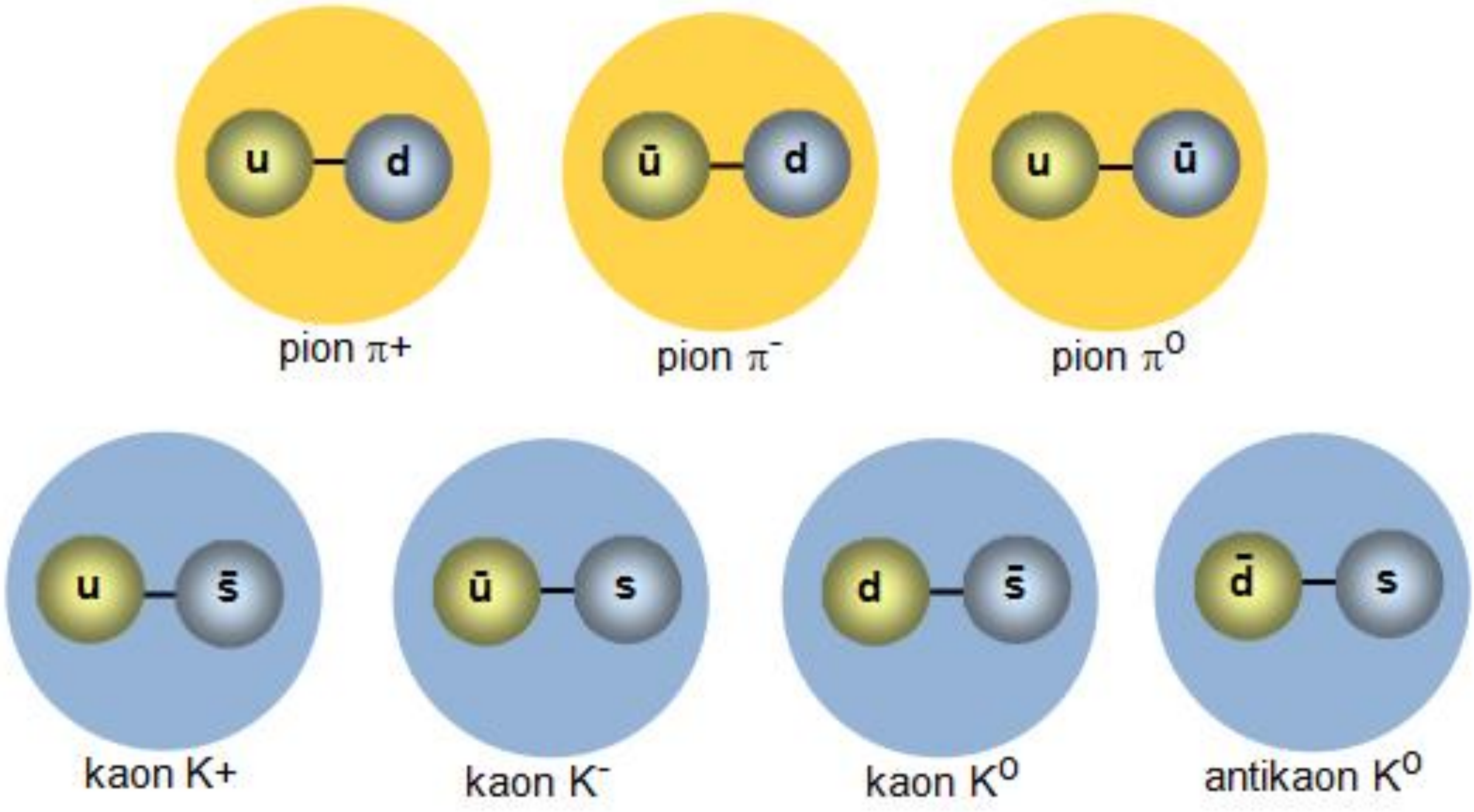

Courtesy of Keith Gibbs. Used with permission.

Galactic Cosmic Ray Origins

"Atmospheric Collision" by User:SyntaxError55, Wikimedia Commons

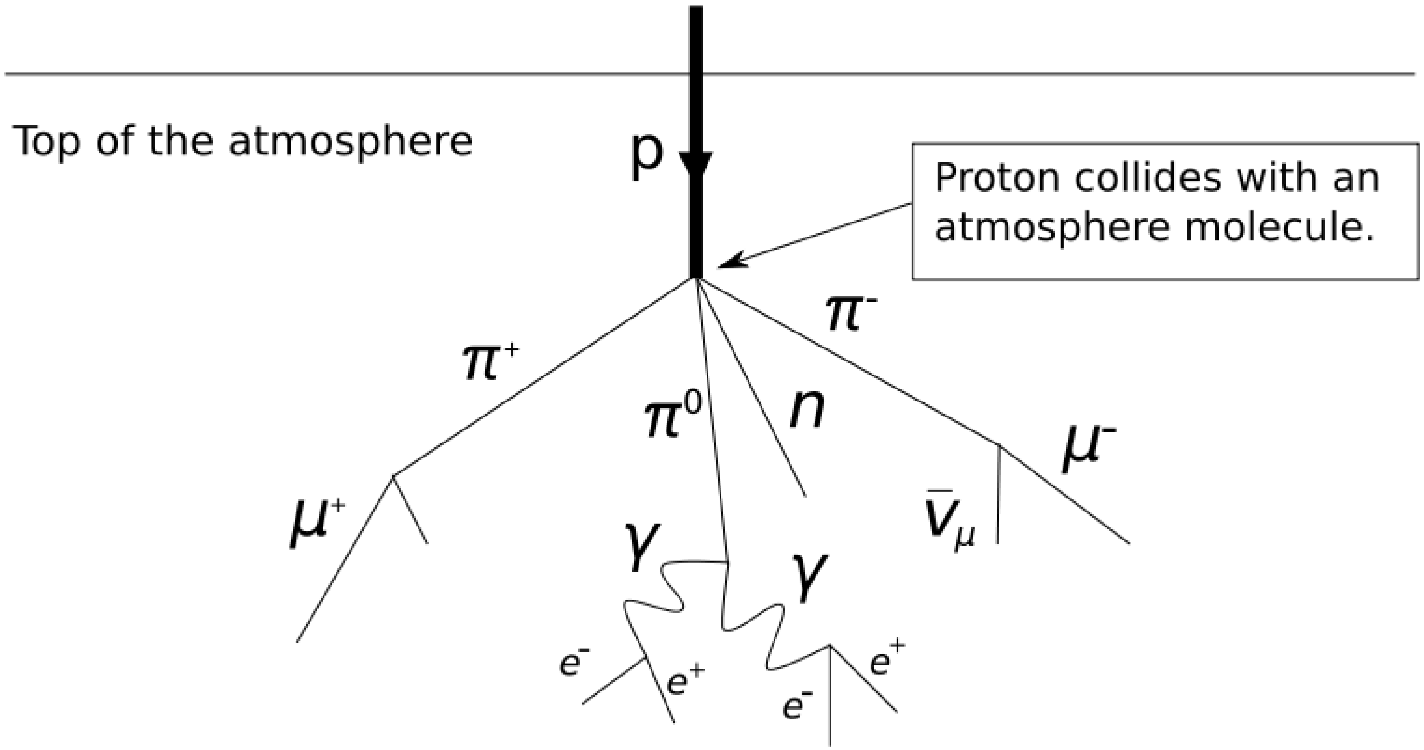

Evidence for Pion Decay

Ackerman, M., et al. *Science* 339 no. 6121 (2013): 807-811
doi:10.1126/science.1231160

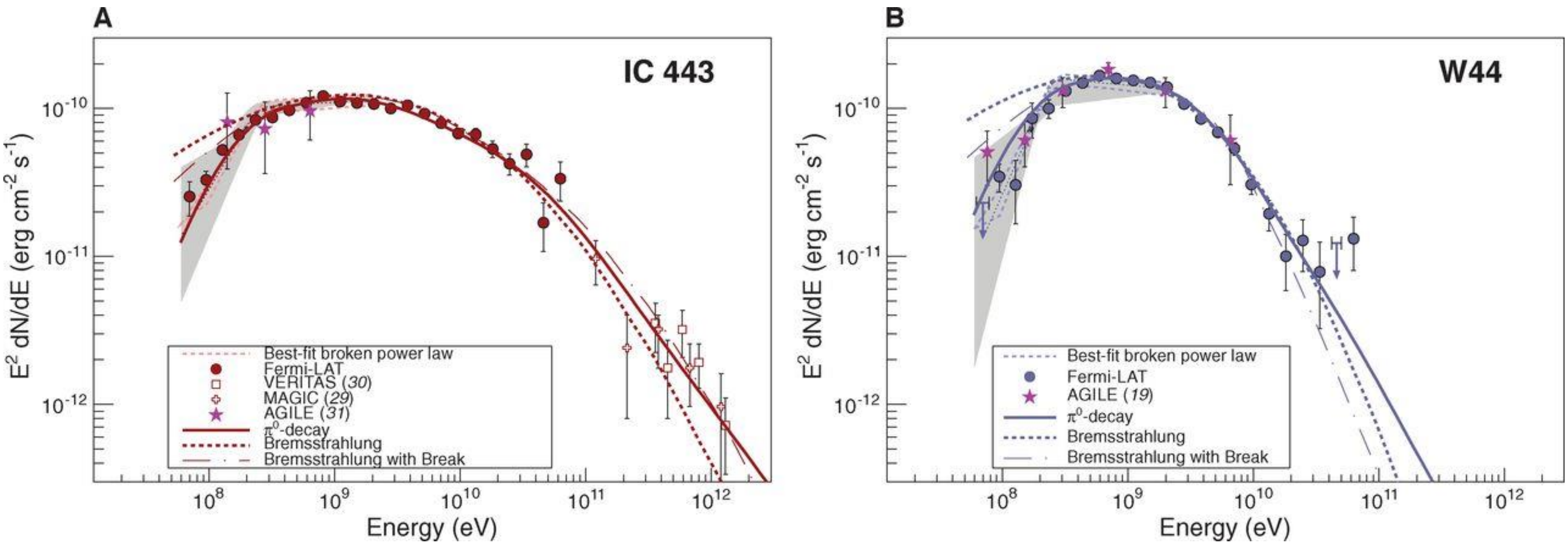

What About Space Travel?

http://photojournal.jpl.nasa.gov/jpeg/PIA17601.jpg

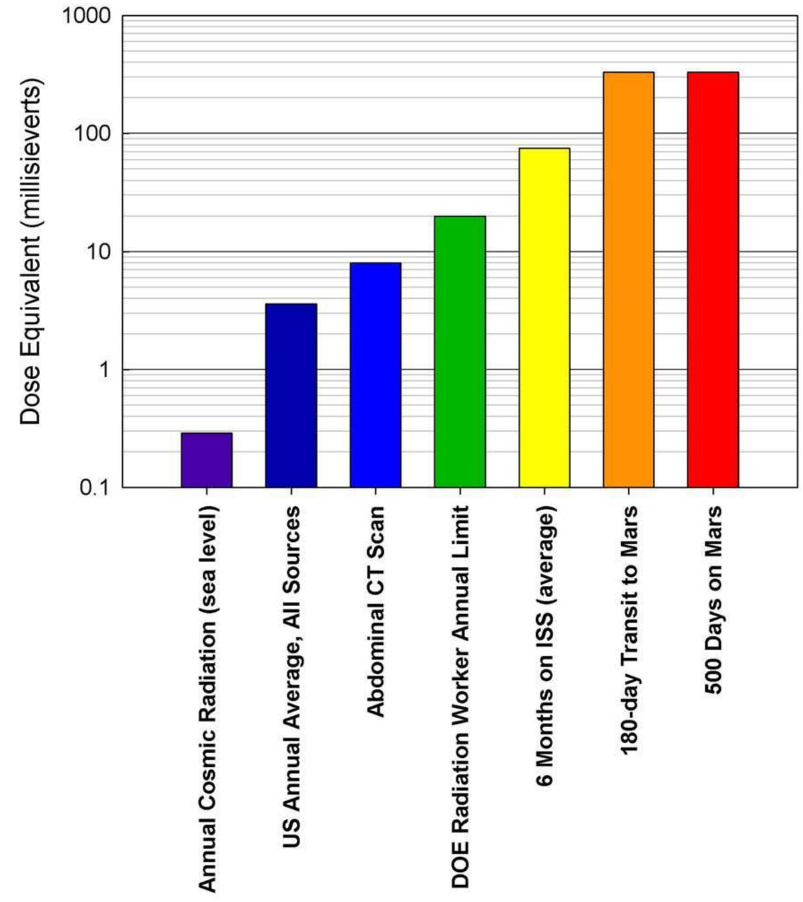

Public domain image, by NASA/JPL-Caltech/SwRI.